Porous Carbon-Faujasite Composites Containing Transition Metals for Aqueous Phase Adsorption Applications

By

Karen M. González-Ramos

A thesis submitted in partial fulfillment of the requirements for the degree of

MASTER OF SCIENCE

in

CHEMICAL ENGINEERING

UNIVERSITY OF PUERTO RICO

MAYAGÜEZ CAMPUS

2014

Approved by:

_____	_____
Arturo Hernández-Maldonado, Ph.D. President, Graduate Committee	Date
_____	_____
María C. Curet-Arana, Ph.D. Member, Graduate Committee	Date
_____	_____
David Suleiman-Rosado, Ph.D. Member, Graduate Committee	Date
_____	_____
Félix R. Román, Ph.D. Member, Graduate Committee	Date
_____	_____
Samuel Hernández-Rivera, Ph.D. Graduate Studies Representative	Date
_____	_____
Aldo Acevedo-Rullán, Ph.D. Chairperson of the Department	Date

Abstract

Pharmaceutical and personal care products (PPCPs) have emerged in surface water in concentration levels enough to categorize them as “emerging contaminants” due to a lack of efficient wastewater treatment plant removal methods. Of several potential alternatives for remediation, only separation via adsorption at ambient conditions eliminates the risk of unwanted side products. The impetus for this contribution is the possibility of combining the hydrophobic nature of carbons with the unique adsorbent-adsorbate interactions provided by a transition metal based faujasite zeolite. A quasi-ordered (CFAU) composite was hydrothermally synthesized and decorated with extraframework transition metal centers (Ni^{2+} or Cu^{2+}). The CFAU variants were fully characterized and performance was assessed via salicylic acid (a high occurrence PPCP) equilibrium adsorption tests at ambient conditions. The salicylic acid equilibrium adsorption capacities increased as follows: FAU < Activated Carbon < CFAU < Ni^{2+}-CFAU << Cu^{2+}-CFAU, proving the synergistic composite is a promising alternative for PPCP remediation.

Resumen

Rastros de productos farmacéuticos y de cuidado personal (PPCP) se han hallado en cuerpos de agua a niveles de concentración lo suficientemente alarmantes para considerarlos como “contaminantes emergentes”. De varias posibles iniciativas para su remoción, sólo el fenómeno de adsorción a condiciones ambientales elimina la posibilidad de productos secundarios. El objetivo de esta contribución es la posibilidad de combinar la naturaleza hidrofóbica del carbón con las interacciones sorbato-sorbente particulares de una zeolita tipo faujasita modificada con metales de transición. Un compuesto semi-ordenado de carbón activado y faujasita (CFAU) fue sintetizado hidrotermálmente y modificado con los metales Ni^{2+} o Cu^{2+}. Las variantes de CFAU fueron caracterizadas y su desempeño establecido mediante pruebas de adsorción en equilibrio de ácido salicílico (un PPCP de alta incidencia) a condiciones ambientales. Las capacidades de adsorción fueron las siguientes: FAU < Carbón Activado < CFAU < Ni^{2+}-CFAU << Cu^{2+}-CFAU, evidenciando que dado al comportamiento sinérgico, CFAU es una alternativa prometedora para la remediación de contaminantes emergentes.

This work is dedicated to my parents for their sacrifice and unconditional support. To my heroes, Abuelos Cuqui and Rafi. To my love for his encouragement, comic reliefs and music. And to my always faithful companion, Luka.

Acknowledgements

This work was possible due to the guidance of my mentor, Dr. Arturo Hernández-Maldonado. My sincere gratitude for his unconditional support and wisdom. Because of him I learned to trust my instincts, that valuable information is obtained from any result, expected or unexpected, and that perseverance is key. I will always value your opinion, support and dedication throughout these years.

My deepest gratitude to my second family, my NSSAL labmates. Thank you for the unconditional support, shared laughs and priceless input. Each of you holds a very special place in my heart. I would also like to acknowledge my undergraduate research assistant, Bethzaely Fernandez, and the members of my graduate committee: professors David Suleiman, María Curet and Felix Román for your time, dedication and valuable suggestions. Particular thanks to Dr. Felix Román for the accessibility and use of his analytical laboratory facility, and Mr. Angel Zapata for his support and words of wisdom.

Finally, I would like to acknowledge the Chemical Engineering Department at the University of Puerto Rico at Mayagüez, the NASA Center for Advanced Nanoscale Materials (CANM) and the National Science Foundation (NSF) under Grant No. HRD 1345156 (CREST Program) for their resources and financial support.

Table of Contents

List of Tables

List of Figures

Chapter 1

Introduction

1.1 Presence and Effects of Contaminants of Emerging Concern in the Environment

During the past few decades, the world has experienced an unprecedented increase in population growth. This accelerated growth has in turn increased both the production and consumption of various materials, especially pharmaceutical and personal care products (PPCPs). In order to satisfy the population's growing demands while meeting their own financial goals, pharmaceutical companies have created products with longer shelf life that contain ingredients that remain active, are resistant to degradation and are highly enduring in aqueous environments. PPCP presence in surface water is attributable to pharmaceutical waste, hospital waste, veterinary medicine, and daily routines. Ingested pharmaceuticals end up in the wastewater system after excretion from the human body; topical materials appear after cleansing and washing, and others by the simple and common act of flushing unused medication directly into

sanitary systems. These products can enter wastewater treatment plants through daily routines, but these plants are unequipped with the materials or methods required to remove PPCPs resulting this in concentrations at least in the parts-per-trillion (ppt) range in surface water, enough to categorize them as "contaminants of emerging concern" (CEC) [1-28].

Although low, recent concentrations are sufficient to potentially affect and impact water quality, ecosystems and human health. It has been reported in literature that present PPCP concentrations may cause potential adverse effects, especially in infants and persons with enzyme deficiencies [29]. Other types of PPCPs or CECs, known as Endocrine Disrupting Chemicals (EDCs), are capable of disrupting the endocrine system, hence hormonal regulation, and directly affecting the health and reproduction capabilities of humans and animals exposed to them [30-33].

1.2 PPCP Remediation Alternatives

Since CECs involve topics of worldwide concern, efforts have been made to further advance water treatment processes, however, such advances are not sufficient or sometimes appropriate for remediation [11, 12, 15, 18, 34-36]. Advanced oxidation processes and ozonation, which are effective processes for PPCP removal from aqueous environments, [37, 38] are either energy intensive or generate unwanted residuals that could create other environmental risks [39, 40]. On the other hand, the process of adsorption has emerged as an alternative to these processes for CEC removal since it requires minimal energy and does not generate potentially harmful residuals.

Several adsorbents are currently being studied and developed for the removal of CECs from aqueous environments. Nanoparticles and nanostructures have drawn the attention of many researchers due to the higher surface area when compared to bulk particles and the advantage

that some can be functionalized with specific chemical groups in order to increase their affinity for target compounds [41, 42]. Selected nanomaterials currently being evaluated include: activated carbon [13, 43, 44], metal-oxide nanoparticles [45], metal organic frameworks [46, 47], coordination polymers [48], clays [49-52], and zeolites [52-58]. Activated carbon (AC) has been the most popular adsorbent for contaminant removal so far due to their hydrophobicity, large capacity and inexpensiveness.

1.3 Adsorbent Selection

Zeolites are microporous materials composed of silicate, aluminosilicate or aluminophosphate crystalline structures. They contain a 3-dimensionally cross-linked framework of aluminum and silicon tetrahedra with cavities that allow for the movement and containment of guest molecules or adsorbates. Extra framework ions balance out the zeolitic framework charges resulting from the alumina tetrahedra. These ions can be easily replaced for others via an ion exchange process in order to provide the zeolite with alternate charges and structural properties that will impart control over the level of material interactions during adsorption of species from gas or liquid phase, hence allowing effective functionalization of the surface and selectivity toward target compounds [59].

Several studies have reported on the occurrence of a phenomenon known as complexation with metals in aqueous environments and PPCPs [60-62]. Complexation is a weak chemical interaction that results from electron donation and backdonation between the *d* and *s* orbitals of a transition metal and an aromatic ring or functional group present in a PPCP or CEC [59, 63]. Exchanging zeolite extra framework ions with transition metals can take advantage of the

complexation phenomena for CEC adsorption which has not yet been used for separation processes and water remediation.

A large selection of CECs contain aromatic rings, however, a regular microporous zeolite (with a maximum pore size of 2 nm) cannot be utilized to remove large compounds due to the small pore size compared to the dugs' molecular dimensions. Furthermore, zeolite pore size can be further reduced after certain functionalization methods. Experimental efforts have been devoted to the development of zeolitic materials with both micropores and mesopores, known as hierarchical materials, in order to take advantage of the zeolite's surface properties [64]. These hierarchical materials allow for greater shape selectivity due to the micropore structures and more efficient mass transfer resulting from the mesopore structure [64]. Some methods for the synthesis of such zeolites include: dealumination, desilication, assembly of zeolite nanocrystals, and soft or hard templating methods, among others [64]. Of these, hard templating methods have proven to be the most promising and precise ones.

Pore size is not the only limitation to CEC adsorption with zeolitic materials. Zeolites are highly hydrophilic materials and aqueous environments could compromise its stability [65]. Due to these limitations, activated carbons (ACs) have been the material of choice in water treatment applications, taking advantage of their hydrophobicity and relatively low cost. However, ACs' surface chemistry is not as flexible as that of zeolitic materials resulting in lower selectivity when compared to the latter [66-70]. Utilizing carbons as hard templates for mesoporous zeolitic composite synthesis could combine the best characteristics of each individual material in a synergistic manner.

1.4 Objectives

The overall objective of this work was the synthesis and characterization of a quasi-ordered carbon-zeolite composite, as well as the synthesis of a three-dimensionally ordered mesoporous carbon for future applications. Faujasite zeolite nanocrystal seeds were prepared using tetramethylammonium hydroxide (TMAOH) as a structure-directing agent. The carbon structure allows for the introduction of mesopores in the composite and also provides the adsorbent with a hydrophobic quality required in an aqueous environment. The hydrophilic zeolite portion of the composite was functionalized via cation exchange with cooper (II) and nickel (II) to allow for complexation type adsorption and hence improve selectivity toward target compounds. The material was further evaluated for the adsorption of salicylic acid, an aromatic PPCP with a high occurrence in surface water [15, 20, 52, 71].

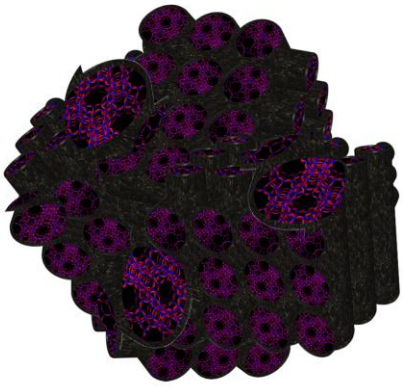

Figure 1.1- Schematic representation of activated carbon-Faujasite composite (CFAU).

Following are the specific objectives:

- Materials syntheses and functionalization
    - Hydrothermal synthesis of quasi-ordered activated carbon-Faujasite composite (CFAU)

- Functionalization of detemplated composite via liquid phase cation exchange with copper and nickel salts
- Synthesis of silica nanoparticles (about 40 nm in diameter)
- Synthesis of a 3-dimensionally ordered mesoporous (3DOm) carbon.

- Material characterization
  - Evaluation of as-synthesized and ion-exchanged materials crystallinity from X-ray diffraction (XRD) data.
  - Determination of elemental composition via thermal gravimetric analysis (TGA) and inductively coupled plasma mass spectroscopy (ICP-MS).
  - Porosimetry analysis of as-synthesized and ion-exchanged materials to estimate textural properties such as surface area, pore size distribution and pore volume.
  - Zeta potential analysis to determine surface charge behavior.
  - X-ray photoelectron spectroscopy (XPS) analysis to determine metal oxidation states.
- Performance test
  - PPCP adsorption experiments using a batch-equilibration technique followed by high performance liquid chromatography (HPLC) analysis to determine the salicylic acid adsorption capacity of each material.

1.5 References

[1] S.G. Alonso, M. Catala, R.R. Maroto, J.L.R. Gil, A.G. de Miguel, Y. Valcarcel. Pollution by psychoactive pharmaceuticals in the rivers of Madrid metropolitan area (Spain). Environ. Int., 36 (2010) 195-201.

[2] H.-R. Buser, M.D. Muller, N. Theobald. Occurrence of the pharmaceutical drug clofibric acid and the herbicide mecoprop in various Swiss lakes and in the North Sea. Environ. Sci. Technol., 32 (1998) 188-192.

[3] V. Calisto, V.I. Esteves. Psychiatric pharmaceuticals in the environment. Chemosphere, 77 (2009) 1257-1274.

[4] C.G. Daughton. Emerging pollutants, and communicating the science of environmental chemistry and mass spectrometry: Pharmaceuticals in the environment. J. Am. Soc. Mass. Spectrom., 12 (2001) 1067-1076.

[5] A.Y.C. Lin, T.H. Yu, S.K. Lateef. Removal of pharmaceuticals in secondary wastewater treatment processes in Taiwan. J. Hazard. Mater., 167 (2009) 1163-1169.

[6] K.C. Makris, S.A. Snyder. Screening of pharmaceuticals and endocrine disrupting compounds in water supplies of Cyprus. Water Sci. Technol., 62 (2010) 2720-2728.

[7] Z. Moldovan. Occurrences of pharmaceutical and personal care products as micropollutants in rivers from Romania. Chemosphere, 64 (2006) 1808-1817.

[8] T.A. Ternes. Occurrence of drugs in German sewage treatment plants and rivers. Water Res., 32 (1998) 3245-3260.

[9] T. Vasskog, U. Berger, P.J. Samuelsen, R. Kallenborn, E. Jensen. Selective serotonin reuptake inhibitors in sewage influents and effluents from Tromso, Norway. J. Chromatogr. A, 1115 (2006) 187-195.

[10] M. Auriol, Y. Filali-Meknassi, R.D. Tyagi, C.D. Adams, R.Y. Surampalli. Endocrine disrupting compounds removal from wastewater, a new challenge. Process Biochem., 41 (2006) 525-539.

[11] D. Bendz, N.A. Paxeus, T.R. Ginn, F.J. Loge. Occurrence and fate of pharmaceutically active compounds in the environment, a case study: Hoje River in Sweden. J. Hazard. Mater., 122 (2005) 195-204.

[12] M. Carballa, F. Omil, J.M. Lema, M. Llompart, C. Garcia, I. Rodriguez, M. Gomez, T. Ternes. Behaviour of pharmaceuticals and personal care products in a sewage treatment plant of northwest Spain. Water Sci. Technol., 52 (2005) 29-35.

[13] L.F. Delgado, P. Charles, K. Glucina, C. Morlay. The removal of endocrine disrupting compounds, pharmaceutically activated compounds and cyanobacterial toxins during drinking water preparation using activated carbon—a review. Sci. Total Environ., 435–436 (2012) 509-525.

[14] M. Grassi, L. Rizzo, A. Farina. Endocrine disruptors compounds, pharmaceuticals and personal care products in urban wastewater: Implications for agricultural reuse and their removal by adsorption process. Environ. Sci. Pollut. Res., 20 (2013) 3616-3628.

[15] M. Gros, M. Petrovic, A. Ginebreda, D. Barcelo. Removal of pharmaceuticals during wastewater treatment and environmental risk assessment using hazard indexes. Environ. Int., 36 (2010) 15-26.

[16] A. Jurado, E. Vazquez-Sune, J. Carrera, M.L. de Alda, E. Pujades, D. Barcelo. Emerging organic contaminants in groundwater in Spain: A review of sources, recent occurrence and fate in a European context. Sci. Total Environ., 440 (2012) 82-94.

[17] B. Kasprzyk-Hordern, R.M. Dinsdale, A.J. Guwy. The removal of pharmaceuticals, personal care products, endocrine disruptors and illicit drugs during wastewater treatment and its impact on the quality of receiving waters (vol 43, pg 363, 2009). Water Res., 44 (2010) 2076-2076.

[18] J.W. Kim, H.S. Jang, J.G. Kim, H. Ishibashi, M. Hirano, K. Nasu, N. Ichikawa, Y. Takao, R. Shinohara, K. Arizono. Occurrence of pharmaceutical and personal care products (PPCPs) in surface water from Mankyung River, South Korea. J. Health Sci., 55 (2009) 249-258.

[19] D.J. Lapworth, N. Baran, M.E. Stuart, R.S. Ward. Emerging organic contaminants in groundwater: A review of sources, fate and occurrence. Environ. Pollut., 163 (2012) 287-303.

[20] J.L. Liu, M.H. Wong. Pharmaceuticals and personal care products (PPCPs): A review on environmental contamination in China. Environ. Int., 59 (2013) 208-224.

[21] I. Muñoz, M.J. Gómez-Ramos, A. Agüera, A.R. Fernández-Alba, J.F. García-Reyes, A. Molina-Díaz. Chemical evaluation of contaminants in wastewater effluents and the environmental risk of reusing effluents in agriculture. Trends Anal. Chem., 28 (2009) 676-694.

[22] A. Pal, K.Y.H. Gin, A.Y.C. Lin, M. Reinhard. Impacts of emerging organic contaminants on freshwater resources: Review of recent occurrences, sources, fate and effects. Sci. Total Environ., 408 (2010) 6062-6069.

[23] S.D. Richardson. Environmental mass spectrometry: Emerging contaminants and current issues. Anal. Chem., 82 (2010) 4742-4774.

[24] S.D. Richardson. Environmental mass spectrometry: Emerging contaminants and current issues. Anal. Chem., 84 (2012) 747-778.

[25] J. Rivera-Utrilla, M. Sanchez-Polo, M.A. Ferro-Garcia, G. Prados-Joya, R. Ocampo-Perez. Pharmaceuticals as emerging contaminants and their removal from water. A review. Chemosphere, 93 (2013) 1268-1287.

[26] S.A. Snyder, M.J. Benotti. Endocrine disruptors and pharmaceuticals: Implications for water sustainability. Water Sci. Technol., 61 (2010) 145-154.

[27] S.A. Snyder, P. Westerhoff, Y. Yoon, D.L. Sedlak. Pharmaceuticals, personal care products, and endocrine disruptors in water: Implications for the water industry. Environ. Eng. Sci., 20 (2003) 449-469.

[28] D.E. Vidal-Dorsch, S.M. Bay, K. Maruya, S.A. Snyder, R.A. Trenholm, B.J. Vanderford. Contaminants of emerging concern in municipal wastewater effluents and marine receiving water. Environ. Toxicol. Chem., 31 (2012) 2674-2682.

[29] T. Heberer. Tracking persistent pharmaceutical residues from municipal sewage to drinking water. J. Hydrol., 266 (2002) 175-189.

[30] S.L. Liu, S.K. Kulp, Y. Sugimoto, J.H. Jiang, H.L. Chang, Y.C. Lin. Involvement of breast epithelial-stromal interactions in the regulation of protein tyrosine phosphatase-gamma (PTP gamma) mRNA expression by estrogenically active agents. Breast Cancer Res. Tr., 71 (2002) 21-35.

[31] S. Jobling, R. Williams, A. Johnson, A. Taylor, M. Gross-Sorokin, M. Nolan, C.R. Tyler, R. van Aerle, E. Santos, G. Brighty. Predicted exposures to steroid estrogens in UK rivers correlate with widespread sexual disruption in wild fish populations. Environ. Health Perspect., 114 (2006) 32-39.

[32] G.S. Prins, L. Birch, W.Y. Tang, S.M. Ho. Developmental estrogen exposures predispose to prostate carcinogenesis with aging. Reprod. Toxicol., 23 (2007) 374-382.

[33] C. Casals-Casas, B. Desvergne. Endocrine disruptors: From endocrine to metabolic disruption. Annu. Rev. Physiol., 73 (2011) 135-162.

[34] T.A. Ternes, J. Stuber, N. Herrmann, D. McDowell, A. Ried, M. Kampmann, B. Teiser. Ozonation: A tool for removal of pharmaceuticals, contrast media and musk fragrances from wastewater? Water Res., 37 (2003) 1976-1982.

[35] A. Joss, S. Zabczynski, A. Gobel, B. Hoffmann, D. Loffler, C.S. McArdell, T.A. Ternes, A. Thomsen, H. Siegrist. Biological degradation of pharmaceuticals in municipal wastewater treatment: Proposing a classification scheme. Water Res., 40 (2006) 1686-1696.

[36] B. Halford. Side effects. Chem. Eng. News, 86 (2008) 13-17.

[37] T.A. Ternes, M. Meisenheimer, D. McDowell, F. Sacher, H.J. Brauch, B.H. Gulde, G. Preuss, U. Wilme, N.Z. Seibert. Removal of pharmaceuticals during drinking water treatment. Environ. Sci. Technol., 36 (2002) 3855-3863.

[38] S. Esplugas, D.M. Bila, L.G.T. Krause, M. Dezotti. Ozonation and advanced oxidation technologies to remove endocrine disrupting chemicals (EDCs) and pharmaceuticals and personal care products (PPCPs) in water effluents. J. Hazard. Mater., 149 (2007) 631-642.

[39] M.M. Huber, S. Korhonen, T.A. Ternes, U. von Gunten. Oxidation of pharmaceuticals during water treatment with chlorine dioxide. Water Res., 39 (2005) 3607-3617.

[40] R. Rosal, A. Rodriguez, M.S. Gonzalo, E. Garcia-Calvo. Catalytic ozonation of naproxen and carbamazepine on titanium dioxide. Appl. Catal., B, 84 (2008) 48-57.

[41] X.L. Qu, J. Brame, Q.L. Li, P.J.J. Alvarez. Nanotechnology for a safe and sustainable water supply: Enabling integrated water treatment and reuse. Acc. Chem. Res., 46 (2013) 834-843.

[42] N. Savage, M. Diallo. Nanomaterials and water purification: Opportunities and challenges. J. Nanopart. Res., 7 (2005) 331-342.

[43] M.S. Mauter, M. Elimelech. Environmental applications of carbon-based nanomaterials. Environ. Sci. Technol., 42 (2008) 5843-5859.

[44] B. Ozkaya. Adsorption and desorption of phenol on activated carbon and a comparison of isotherm models. J. Hazard. Mater., 129 (2006) 158-163.

[45] S. Ghosh, A.Z.M. Badruddoza, K. Hidajat, M.S. Uddin. Adsorptive removal of emerging contaminants from water using superparamagnetic Fe_3O_4 nanoparticles bearing aminated β-cyclodextrin. J. Environ. Chem. Eng., 1 (2013) 122-130.

[46] Z. Hasan, E.J. Choi, S.H. Jhung. Adsorption of naproxen and clofibric acid over a metal-organic framework MIL-101 functionalized with acidic and basic groups. Chem. Eng. J., 219 (2013) 537-544.

[47] N.A. Khan, Z. Hasan, S.H. Jhung. Adsorptive removal of hazardous materials using metal-organic frameworks (MOFs): A review. J. Hazard. Mater., 244 (2013) 444-456.

[48] K.A. Cychosz, A.J. Matzger. Water stability of microporous coordination polymers and the adsorption of pharmaceuticals from water. Langmuir, 26 (2010) 17198-17202.

[49] W.A. Cabrera-Lafaurie, F.R. Román, A.J. Hernández-Maldonado. Transition metal modified and partially calcined inorganic–organic pillared clays for the adsorption of salicylic acid, clofibric acid, carbamazepine, and caffeine from water. J. Colloid Interface Sci., 386 (2012) 381-391.

[50] W.A. Cabrera-Lafaurie, F.R. Román, A.J. Hernández-Maldonado. Single and multi-component adsorption of salicylic acid, clofibric acid, carbamazepine and caffeine from water

onto transition metal modified and partially calcined inorganic–organic pillared clay fixed beds. J. Hazard. Mater., (2014) 1-9.

[51] S.M. Rivera-Jimenez, M.M. Lehner, W.A. Cabrera-Lafaurie, A.J. Hernandez-Maldonado. Removal of naproxen, salicylic acid, clofibric acid, and carbamazepine by water phase adsorption onto inorganic-organic-intercalated bentonites modified with transition metal cations. Environ. Eng. Sci., 28 (2011) 171-182.

[52] V. Rakic, N. Rajic, A. Dakovic, A. Auroux. The adsorption of salicylic acid, acetylsalicylic acid and atenolol from aqueous solutions onto natural zeolites and clays: Clinoptilolite, bentonite and kaolin. Microporous Mesoporous Mater., 166 (2013) 185-194.

[53] W.A. Cabrera-Lafaurie, F.R. Román, A.J. Hernández-Maldonado. Removal of salicylic acid and carbamazepine from aqueous solution with Y-zeolites modified with extraframework transition metal and surfactant cations: Equilibrium and fixed-bed adsorption. J. Environ. Chem. Eng., 2 (2014) 899-906.

[54] J.E. Krohn, M. Tsapatsis. Phenylalanine and arginine adsorption in zeolites X, Y, and Beta. Langmuir, 22 (2006) 9350-9356.

[55] A. Martucci, L. Pasti, N. Marchetti, A. Cavazzini, F. Dondi, A. Alberti. Adsorption of pharmaceuticals from aqueous solutions on synthetic zeolites. Microporous Mesoporous Mater., 148 (2012) 174-183.

[56] D.J. de Ridder, J. Verberk, S.G.J. Heijman, G.L. Amy, J.C. van Dijk. Zeolites for nitrosamine and pharmaceutical removal from demineralised and surface water: Mechanisms and efficacy. Sep. Purif. Technol., 89 (2012) 71-77.

[57] B. Koubaissy, G. Joly, I. Batonneau-Gener, P. Magnoux. Adsorptive removal of aromatic compounds present in wastewater by using dealuminated faujasite zeolite. Ind. Eng. Chem. Res., 50 (2011) 5705-5713.

[58] A. Rossner, S.A. Snyder, D.R.U. Knappe. Removal of emerging contaminants of concern by alternative adsorbents. Water Res., 43 (2009) 3787-3796.

[59] R.T. Yang, Adsorbents: Fundamentals and applications., Wiley, New York, 2003.

[60] R. Cini, G. Tamasi, S. Defazio, M.B. Hursthouse. Unusual coordinating behavior by three non-steroidal anti-inflammatory drugs from the oxicam family towards copper(II). Synthesis, X-ray structure for copper(II)-isoxicam, -meloxicam and -cinnoxicam-derivative complexes, and cytotoxic activity for a copper(II)-piroxicam complex. J. Inorg. Biochem., 101 (2007) 1140-1152.

[61] D. Kovala-Demertzi. Recent advances on non-steroidal anti-inflammatory drugs, NSAIDS: Organotin complexes of nsaids. J. Organomet. Chem., 691 (2006) 1767-1774.

[62] J.E. Weder, C.T. Dillon, T.W. Hambley, B.J. Kennedy, P.A. Lay, J.R. Biffin, H.L. Regtop, N.M. Davies. Copper complexes of non-steroidal anti-inflammatory drugs: An opportunity yet to be realized. Coord. Chem. Rev., 232 (2002) 95-126.

[63] S.M. Rivera-Jimenez, A.J. Hernandez-Maldonado. Nickel(II) grafted MCM-41: A novel sorbent for the removal of naproxen from water. Microporous Mesoporous Mater., 116 (2008) 246-252.

[64] H.Y. Chen, J. Wydra, X.Y. Zhang, P.S. Lee, Z.P. Wang, W. Fan, M. Tsapatsis. Hydrothermal synthesis of zeolites with three-dimensionally ordered mesoporous-imprinted structure. J. Am. Chem. Soc., 133 (2011) 12390-12393.

[65] K.Y. Foo, B.H. Hameed. The environmental applications of activated carbon/zeolite composite materials. Adv. Colloid Interface Sci., 162 (2011) 22-28.

[66] S.A. Snyder, M.J. Benotti. Endocrine disruptors and pharmaceuticals: Implications for water sustainability. Water Sci. Technol., 61 (2010) 145.

[67] C. Adams, Y. Wang, K. Loftin, M. Meyer. Removal of antibiotics from surface and distilled water in conventional water treatment processes. J. Environ. Eng., 128 (2002) 253-260.

[68] P. Westerhoff, Y. Yoon, S. Snyder, E. Wert. Fate of endocrine-disruptor, pharmaceutical, and personal care product chemicals during simulated drinking water treatment processes. Environ. Sci. Technol., 39 (2005) 6649-6663.

[69] S.A. Snyder, S. Adham, A.M. Redding, F.S. Cannon, J. DeCarolis, J. Oppenheimer, E.C. Wert, Y. Yoon. Role of membranes and activated carbon in the removal of endocrine disruptors and pharmaceuticals. Desalination, 202 (2007) 156-181.

[70] Z. Yu, S. Peldszus, P.M. Huck. Adsorption of selected pharmaceuticals and an endocrine disrupting compound by granular activated carbon: 1. Adsorption capacity and kinetics. Environ. Sci. Technol., 43 (2009) 1467-1473.

[71] J. Huang, G. Wang, K. Huang. Enhanced adsorption of salicylic acid onto a β-naphthol-modified hyper-cross-linked poly (styrene-co-divinylbenzene) resin from aqueous solution. Chem. Eng. J., 168 (2011) 715-721.

Chapter 2

A Hierarchical Porous Carbon-M^{n+}[FAU] (M^{n+} = Ni^{2+} or Cu^{2+}) Adsorbent: Synthesis, Characterization and Adsorption of Salicylic Acid from Water

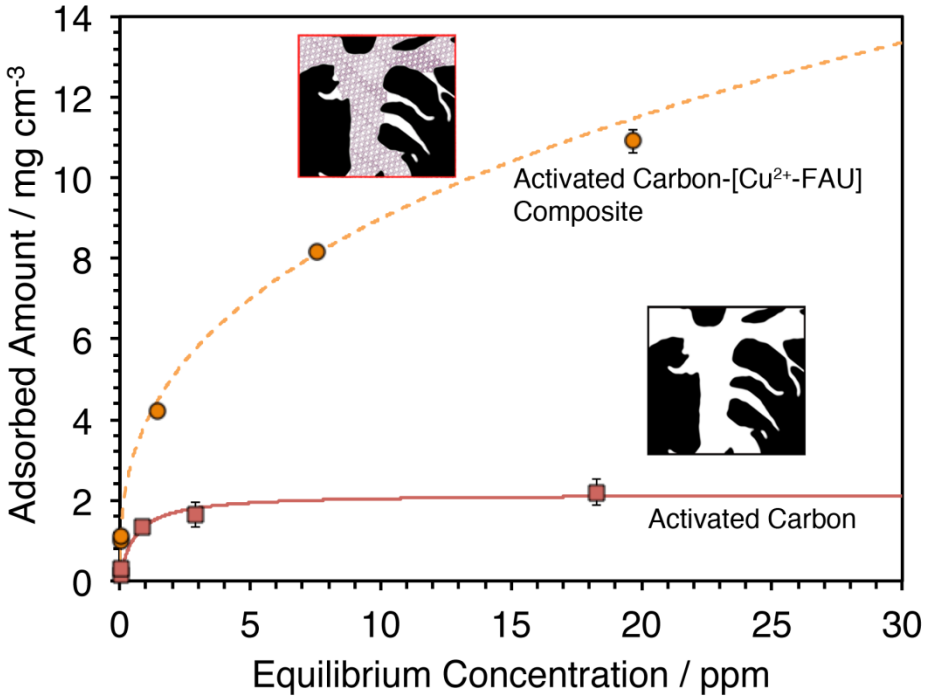

2.1 Introduction

Increased efforts have arisen in the area of bottom-up design of adsorbent materials with flexible and easily manipulated surfaces that allow for specific interactions with adsorbates. Tailored adsorbents allow for selective separation of particular compounds from a medium, deeming it a viable alternative for the removal of contaminants of emerging concern (CECs) present in water at low concentrations, a topic of worldwide concern [1-12]. CECs include pharmaceutical and personal care products (PPCPs) and

endocrine disrupting chemicals (EDCs). However, challenges arise in the ability to design a hydrophobic adsorbent platform, stable in aqueous environments, with the desired surface flexibility and interactions.

Several adsorbents have been considered for the removal of CECs from aqueous environments. Nanoparticles and nanostructures, for instance, have drawn much attention due to the higher surface area when compared to bulk particles [13]. Selected materials that have been evaluated include: activated carbon [14-16], metal-oxide nanoparticles [17], metal organic frameworks [18, 19], coordination polymers [20], clays [21-24], and zeolites [23, 25-30]. So far, activated carbon (AC) has been the adsorbent of choice for water remediation due to its hydrophobicity, large capacity and relative low cost. However, AC's surface chemistry is not as flexible as that of other materials, deeming it an unsuitable platform for surface functionalization and hence resulting in lower selectivity toward specific adsorbates present in complex mixtures [4, 31-34].

Hernández-Maldonado and coworkers have reported on the synthesis and performance of transition metal based clays [21, 22, 24], mesoporous silica [35, 36], and zeolites [30], all designed to increase affinity toward target CECs. Zeolites based on aluminosilicate frameworks have extra framework metal cations that balance out the framework charges. These can be easily replaced for others via ion exchange processes in order to provide the zeolite with alternate surface charges and structural properties that will impart control over the level of adsorption interactions during the uptake of species from liquid phases, hence allowing effective functionalization of the surface and selectivity toward target compounds [37]. One such method for the adsorption of target compounds could be achieved via a complexation process between the *d* and *s* orbitals of

a transition metal ion in the zeolite and the aromatic ring and/or functional groups of an organic adsorbate through electron donation and backdonation [38-40]. Studies have demonstrated PPCP complexation with metals in aqueous solutions [41-43], however such a phenomenon has not yet been used for separation processes or water remediation. In addition, complexation-like PPCP-adsorbent interactions should be deemed weak in the sense that the adsorbent could be regenerated with minimal energy consumption and simple engineering means.

Although zeolites exhibit a flexible surface chemistry, limitations arise regarding its stability and pore size. Zeolites based on aluminosilicate frameworks are highly hydrophilic materials and aqueous environments could even compromise its stability [44]. In addition, bulky molecules with diameters greater than 2 nm are excluded from interactions that occur within the supercages of zeolites such as Faujasite (FAU) [39]. However, utilizing carbons as hard templates for zeolite crystal growth [45] could combine the best characteristics of each individual material in a synergistic manner and tackle the limitations associated to hydrophobicity and surface flexibility for functionalization or tailoring. Chen and coworkers have reported on the growth of zeolites within three-dimensionally ordered mesoporous carbons to yield zeolites with imprinted mesoporosity after carbon template removal [45]. However, the removal of the carbon template will certainly result in a loss of the material hydrophobic properties. Others have synthesized activated carbon zeolite composites by converting coal fly ash directly into the composite via fusion and hydrothermal treatment, primarily for the removal of heavy metals from wastewater [46, 47].

The overall objective of this work was the synthesis and characterization of a quasi-ordered hierarchical porous carbon-FAU (CFAU) material or composite by mixing zeolite seeds with activated carbon. Y zeolite (FAU) zeolite nanocrystal seeds were prepared using a structure directing agent (SDA; tetramethylammonium hydroxide, TMAOH) and proper aging times [45, 48-50]. The carbon structure allows for the introduction of mesopores in the composite and also provides the adsorbent with a hydrophobic quality required in an aqueous environment. The hydrophilic FAU portion of the composite was effectively functionalized via cation exchange with copper(II) and nickel(II) to allow for the possibility of complexation-like adsorption and hence improve selectivity toward a target compound over water. The hierarchical porous material and its transition metal containing variants were each evaluated for the adsorption of salicylic acid, an aromatic PPCP with a high occurrence in surface water [3, 11, 23, 51].

2.2 Experimental Section

2.2.1 Reagents and Materials

Reagents used for the synthesis and postsynthesis modifications of the hierarchical materials or composites were the following: distilled/deionized water, aluminum isopropoxide (98%), tetramethylammonium hydroxide (TMAOH, 25 wt. %), Ludox HS-40 colloidal silica (40 wt. % suspension in H_2O), activated carbon (Darco KB-G, Norit), nickel(II) sulfate hexahydrate (puriss. p.a., ACS reagent, 99-102%,), copper(II) nitrate hemi(pentahydrate) (99.99%), nickel(II) chloride hexahydrate (99.999%), copper(II) nitrate trihydrate (puriss. p.a., 99-104%), dimethylformamide (DMF, anhydrous, 99.8%), and salicylic acid (99%). All materials, with the exception of water and the activated

carbon, were obtained from Sigma-Aldrich and used as received. The activated carbon (Darco-KB) was obtained from Norit Inc.

2.2.2 Synthesis of the Hierarchical Material

The carbon-FAU composite, CFAU, was synthesized via hydrothermal crystallization using tetramethylammonium hydroxide (TMAOH) as the structure directing agent with an initial gel composition of $10.0SiO_2$:$2.30Al_2O_3$:$5.50(TMA)_2O$:$0.10Na_2O$:$570H_2O$. Similar synthesis procedures have been reported elsewhere, but utilizing a three-dimensionally ordered mesoporous carbon instead of activated carbon [45]. Aluminum isopropoxide, TMAOH and deionized water were mixed at room temperature for 90 minutes. Ludox HS-40 was added dropwise. After aging for 24 hours, activated carbon was added and the resulting synthesis gel was transferred to a Teflon-lined vessel and heated for 4 days at 100 ˚C under autogenous conditions. The growth process was repeated 5 times and the final material was recovered via vacuum filtration, washed with copious amounts of deionized water and oven-dried at 70 ˚C. Template removal was achieved after calcination at 550 ˚C in a furnace for 12 hours under pure nitrogen flow.

2.2.3 Post-synthesis Transition Metal Ion Exchange

Transition metal based M^{n+}-CFAU (M^{n+} = Ni^{2+} or Cu^{2+}) composites were prepared via cation exchange on the detemplated CFAU (i.e., H^+,Na^+-CFAU) composite in liquid phase varying the solvent with the respective salts containing the desired cation (Ni^{2+} or Cu^{2+}). Metal salts, nickel(II) sulfate hexahydrate or copper(II) nitrate hemi(pentahydrate), were dissolved in 200 mL distilled/deionized water (0.6 mg/mL) at

80 ˚C. Metal salts, nickel(II) chloride hexahydrate and copper(II) nitrate trihydrate, were also dissolved in 200 mL DMF (1.1 mg/mL) at 100 ˚C. The required salt quantities were determined according to the cation exchange capacity of the synthesized FAU zeolite. Excess loadings were used to guarantee maximum ion exchange. In a typical experiment, 0.5 g of the composite, containing 0.28 g FAU, were added to the aforementioned transition metal salt solutions and stirred for 24 hours. The resulting suspensions were then centrifuged and washed several times with copious amounts of distilled/deionized water followed by drying at 60 ˚C. These materials will be referred to as Ni^{2+}-CFAU (W), Cu^{2+}-CFAU (W), Ni^{2+}-CFAU (D), Cu^{2+}-CFAU (D), where the "W" and "D" correspond to the materials exchanged in water and DMF respectively.

2.2.4 Characterization Methods

X-ray powder diffraction (XRD) patterns were collected on a Rigaku Ultima III diffractometer using CuKα radiation (λ = 1.5418 Å) operating at 40 kV and 44mA. Patterns were obtained with a scanning speed of 1°/min and a step of 0.02˚ on a 2θ range of 5-50˚. Weight loss profiles as a function of temperature were obtained using a TA-Q500 thermogravimetric analyzer (TGA). These data were used to estimate the physisorbed water and template (TMA^+) content of the samples. The TGA was operated with an inert gas (helium) at a flow rate of 60 mL min^{-1} while heating the samples from room temperature to 900 ˚C at a rate of 10 ˚C min^{-1}. The sample gas was pretreated with presorbers to remove traces of water prior to entering the analyzer's gas chamber.

Chemical compositional data for the samples were gathered using inductively coupled plasma mass spectroscopy (ICP-MS). These tests were performed in the Galbraith Laboratories, Inc. facilities in Knoxville, TN, USA. Surface charge profiles

were estimated using zeta potential data obtained with a Brookhaven Instruments ZetaPlus unit. All the composite materials were suspended in water (0.2% w/v) and zeta potential measurements were collected at pH values in the 2 - 12 range. A constant ionic strength was maintained during tests via a 0.001 M KCl concentration solution.

Metal oxidation states on the M^{n+}-CFAU samples were assessed via X-ray photoelectron spectroscopy (XPS) performed on a PHI Versa Probe (II) 5000 unit with monochromatized AlKα radiation ($h\nu$ = 1486.6 eV) and with binding energies calibrated with respect to C1s peak (284.5 eV). Samples were preserved under vacuum for 2 hours in the intro chamber prior to analysis.

Textural properties were determined via a porosimetry analysis of nitrogen adsorption equilibrium data gathered at -196 ˚C in a Micromeritics ASAP 2020 static volumetric adsorption unit fitted with turbomolecular pumps. Prior to each analysis, the samples were degassed under vacuum at 250 ˚C for 16 hours. The activated samples were always transferred from the degas to the analysis ports in glass vials fitted with isolation valves to avoid exposure to ambient. The data were utilized to estimate the surface area and pore volume of the detemplated CFAU samples. Surface areas were estimated using the BET isotherm model while the pore volume was estimated using the Horvath-Kawazoe approach [52, 53].

2.2.5 Salicylic Acid Adsorption Equilibrium Isotherms

Adsorption equilibrium isotherm data for salicylic acid were gathered using a batch equilibration technique. In a typical test, 0.015 g of the adsorbent were mixed with 15 mL of the aqueous salicylic acid solution at various concentrations (0.1 - 30 ppm) in 50 mL borosilicate centrifuge tubes. The solution pH for each concentration was adjusted to 10

and 4 for the activated carbon and the composites respectively in order to reach a final nearly neutral equilibrium pH (7-8 range) and better simulate conditions found in typical water treatment plants. The tubes were shaken for 24 hours at room temperature and then centrifuged at 8500 rpm for 5 minutes to recover the aqueous phase. The experiment was conducted in triplicates and the salicylic acid concentration was estimated using a high performance liquid chromatography (HPLC) system (Agilent 1100 Series HPLC module) with a diode array detector (DAD) fitted with a deuterium lamp and a temperature control unit. The adsorbate was separated from the aqueous solution with a Zorbax Eclipse XDB Column C8 using an acetonitrile/(water 1% folic acid) mixture at a composition of 30:70 and a flow rate of 1.0 mL/min. Salicylic acid adsorbed amounts were calculated based on concentration differences (i.e., mass balances). A similar procedure was employed to determine salicylic acid uptakes as a function of time. Solutions of 1 and 8 ppm were prepared, mixed with 0.015 g of composite, and shaken at room temperature for 28 hours. Small aliquots were taken at various time intervals and plotted to verify that 24 hours was sufficient to achieve equilibrium.

The equilibrium adsorption isotherm data were fitted with Langmuir (2.1), Freundlich (2.2), or Sips (2.3) isotherm models:

$$\frac{q}{q_{mL}} = \frac{k_L C_E}{1 + k_L C_E} \tag{2.1}$$

$$q = k_F C_E^{\,1/n_F} \tag{2.2}$$

$$\frac{q}{q_{mS}} = \frac{k_S C_E^{\,1/n_s}}{1 + k_S C_E^{\,1/n_s}} \tag{2.3}$$

where q is the salicylic acid amount adsorbed at equilibrium with an aqueous concentration C_E, q_m is the salicylic acid maximum adsorbed amount, k is an interaction parameter for each particular model, and n is a semi-quantitative surface descriptor that accounts for surface heterogeneity.

2.3 Results and Discussion

2.3.1 Structural, Textural and Compositional Analyses

The crystallinity of the zeolitic component (i.e., Y zeolite) of the CFAU hierarchical material or composite was verified with XRD patterns for both the as-synthesized and transition metal containing samples (Fig. 2.1). Faujasite crystallinity was conserved after incorporation of the activated carbon in the synthesis gel as observed from the XRD patterns corresponding to CFAU. However, it should be noted that a negligible amount of LTA phase was also present in the sample as suggested by the peak at 7.2˚. Based on relative diffraction intensities for each characteristic peak only ca. 9 % corresponded to an LTA phase. SEM images of the sample (Fig. A-2) were also used to analyze purity and estimates suggest an LTA impurity of ca. 9 %, which correlates well with XRD data.

Crystallinity was generally conserved after inclusion of Ni^{2+} and Cu^{2+} into CFAU as evidenced by both XRD patterns as well as the consistency of samples surface areas (see Table 2.1). However, there is a noticeable decrease in the intensity of FAU characteristic peaks at 6.14, 10 and 11.7˚ corresponding to planes (1 1 1), (2 2 0) and (3 1 1), respectively. The modified intensities may be attributed to diffraction from a secondary metal lattice in the presence of coordinated water [54]. The formation of this secondary lattice could occur as long as the framework aluminum atoms are distributed in an orderly

fashion [54]. The peak intensities decreased further for the CFAU samples exchanged in water, which may suggest a larger quantity of water molecules present within the FAU structure. This is also evident in the composition data shown in Table 2.1.

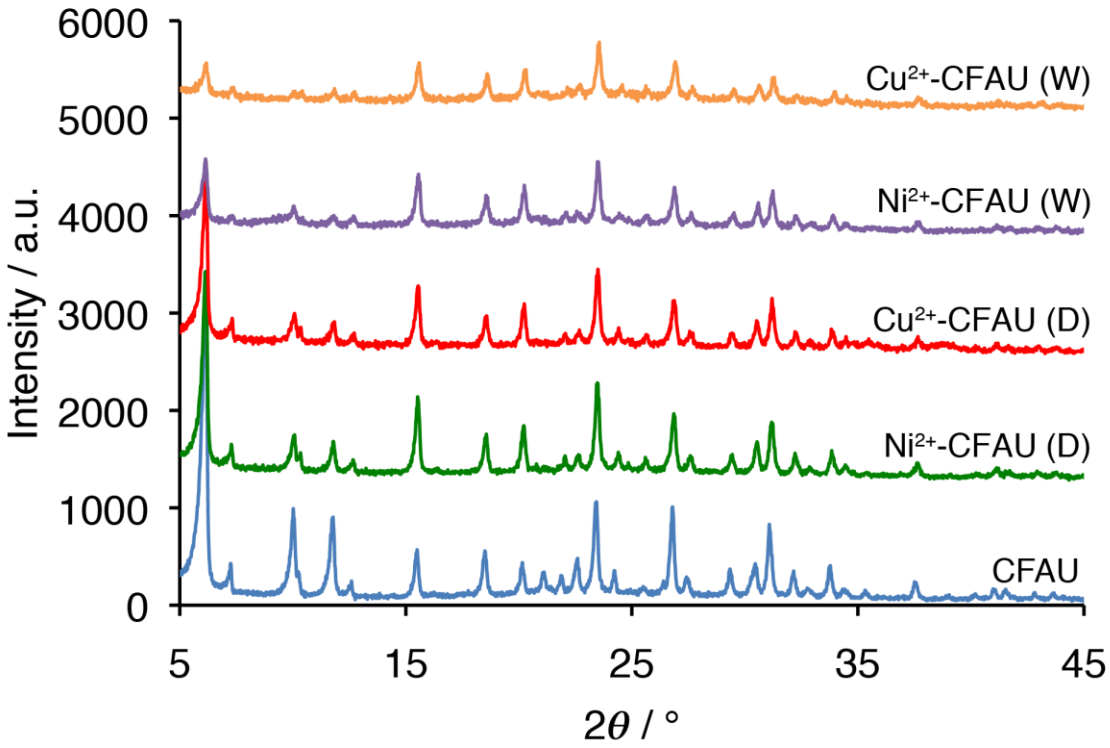

Figure 2.1 - X-ray diffraction patterns for detemplated CFAU and transition metal (Cu^{2+} and Ni^{2+}) cation exchanged CFAU. Ion exchange was performed in either water (W) or dimethylformamide (D). The peak at ~7.4° corresponds to traces of a LTA phase.

TGA weight loss profiles for as-synthesized and detemplated CFAU can be observed in Fig. 2.2 (top). Portions of the contents of as-synthesized CFAU decompose in three steps. The first weight loss corresponds to desorption of water molecules. The second and third weight losses at 213 and 487 ˚C are ascribed to the decomposition of the template TMA^+ present in the supercage and sodalite cages of the FAU structure, respectively. TMA^+ located within the sodalite cage is more constricted, hence the higher decomposition temperature [49]. Upon calcination, the zeolite portion of CFAU exhibits only one weight loss step corresponding to desorption of water molecules. Complete

template decomposition was achieved after calcination and the overall structural charges were balanced by Na^+, and H^+ ions left behind after TMA^+ breakdown (i.e., H^+,Na^+-CFAU). Fig. 2.2 (bottom) contains the TGA weight loss profiles for the transition metal ion exchanged composites (i.e., M^{n+}-CFAU). The decomposition of the contents of the transition metal containing composites prepared via ion exchange in water, Cu^{2+}-CFAU (W) and Ni^{2+}-CFAU (W), follows a step-wise mechanism similar to that of the H^+,Na^+-CFAU, with only one weight loss step showing before 200 ˚C and related to the desorption of water. The materials prepared via ion exchange in DMF, Cu^{2+}-CFAU (D) and Ni^{2+}-CFAU (D), exhibited the same first water desorption weight loss step and another weight loss step at 350 ˚C. It is highly unlikely that this weight loss is due to TMA^+ since ion exchange took place after template removal and, as noted in Fig. 2.2 (top), upon calcination at 550 ˚C the sample had no traces of TMA^+. Therefore, the weight loss step observed at 350 ˚C probably corresponded to breakdown of DMF that may still be present well within the pores of the composite structure, and hence the higher decomposition temperature.

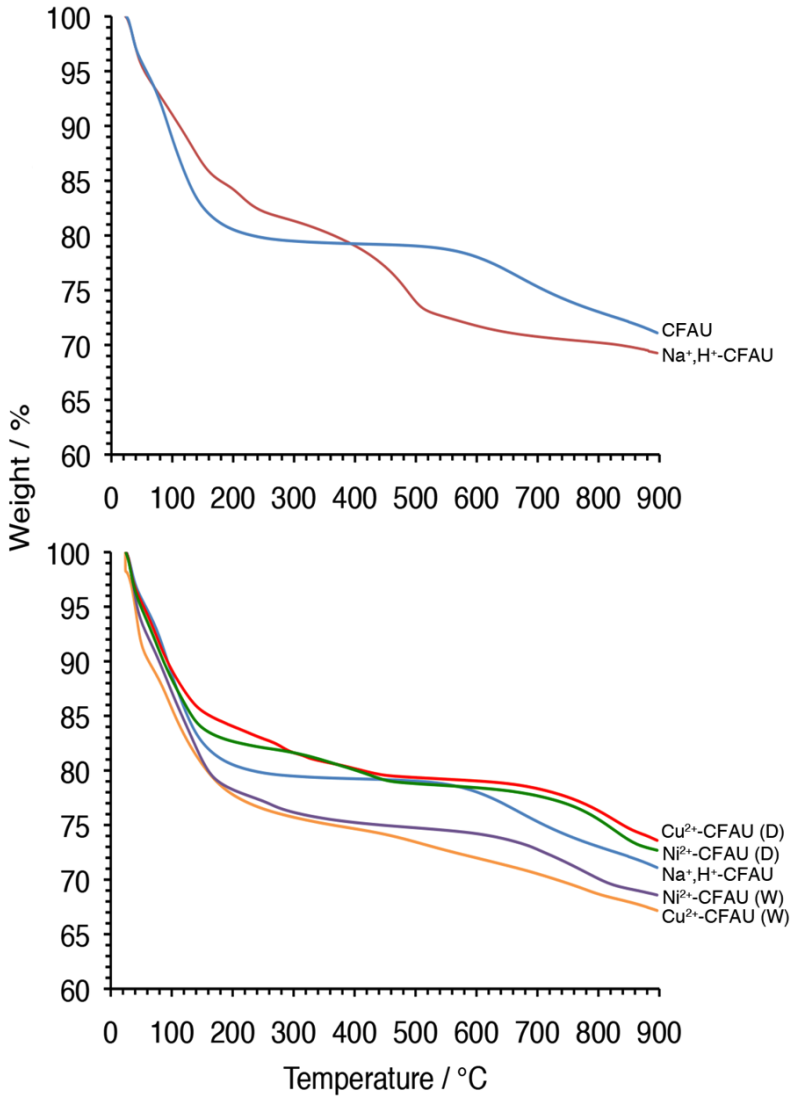

Figure 2.2 - Weight loss profiles for as synthesized CFAU and Na^{+},H^{+}-CFAU after calcination (*top*) and for transition metal (Cu^{2+} and Ni^{2+}) cation exchanged CFAU (*bottom*). Ion exchange was performed in either water (W) or dimethylformamide (D).

A summary of the textural properties of all the composites is presented in Table 2.1. Surface area was tabulated as an overall BET surface area, as well as surface area contributions for activated carbon and FAU, which were calculated for each composite based on the weight fractions of each material. As expected, the BET surface area decreases considerably upon FAU growth within the activated carbon voids. The surface area decreases further after ion exchange since the exchanged metals are larger than the

H^+ and Na^+ ions originally present in the detemplated CFAU. A similar observation can be made for the composites exchanged in DMF, which corroborates the hypothesis from the TGA analysis that DMF is still present within the pores of the composite. Pore volume and size data followed the same trend as that for surface area. However, it should be noted that activated carbon, as well as the composites are non-ordered structures that possess macropores, mesopores and micropores, hence they lack a well-defined Gaussian type pore size distribution.

The unit cell FAU chemical compositions shown in Table 2.1 were determined via ICP-MS spectroscopy in conjunction with the TGA data. In general, the Si/Al ratio was slightly affected after functionalization or ion exchange of the CFAU samples. A plausible explanation for this could be that the composition of the Cu^{2+}-CFAU (W) and Ni^{2+}-CFAU (W) may have been affected by the acidic levels of the ion exchange (pH 5.77 and 5.01 respectively) resulting in a slightly lower Si/Al ratios. In addition, it seems that for Cu^{2+}-CFAU (D), H^+ was preferentially exchanged by Cu^{2+}. This may be due to the larger size of the DMF molecule compared to that of the water molecule; it would preferentially enter and transport Cu^{2+} through less constricted areas where H^+ is present and not the larger Na^+. However, there was very little exchange with Ni^{2+} suggesting that perhaps DMF does not solvate and transport Ni^{2+} as effectively as Cu^{2+}. Finally, there is a larger amount of water in the Cu^{2+}-CFAU (W) and Ni^{2+}-CFAU (W) materials, which corroborates the XRD analysis assumption that water molecules present in the structure could result in a decrease in the intensity of the characteristic peaks.

Table 2.1 - Textural properties of activated carbon (AC) and CFAU samples. Transition metals were exchanged in water (W) or dimethylformamide (D).

Adsorbent	Unit Cell Compositon[a]	Porosimetry			
		BET SA (m^2/g)[b]	AC_{SA} (m^2/g)	FAU_{SA} (m^2/g)	Pore Volume (cm^3/g)[c]
AC	-	1258	-	-	1.126
Na^+, H^+-CFAU	$Na_{33.93}\ H_{30.07}\ [Al_{64}\ Si_{113}\ O_{384}]\ *178.67\ H_2O$	559	246	313	0.412
Cu^{2+}-CFAU (W)	$Na_{5.13}\ Cu_{14.00}\ H_{37.79}\ [Al_{70.92}\ Si_{109.01}\ O_{384}]\ *229.13\ H_2O$	527	232	295	0.442
Ni^{2+}-CFAU (W)	$Na_{8.50}\ Ni_{12.89}\ H_{30.46}\ [Al_{64.75}\ Si_{99.28}\ O_{384}]\ *218.85\ H_2O$	532	234	298	0.424
Cu^{2+}-CFAU (D)	$Na_{21.41}\ Cu_{17.09}\ H_{6.52}\ [Al_{62.11}\ Si_{111.84}\ O_{384}]\ *136.98\ H_2O\ *10.31\ DMF$	463	204	259	0.369
Ni^{2+}-CFAU (D)	$Na_{25.31}\ Ni_{3.93}\ H_{28.94}\ [Al_{62.11}\ Si_{116.93}\ O_{384}]\ *151.38\ H_2O\ *6.513\ DMF$	417	183	234	0.318

[a] From ICP-MS and TGA measurements
[b] From N_2 equilibrium adsorption isotherms gathered at -196 ˚C
[c] From N_2 equilibrium adsorption isotherms gathered at -196 ˚C and a Horvath-Kawazoe approach

2.3.2 Salicylic Acid Adsorption Performance

Prior to the salicylic acid adsorption performance tests, it was necessary to perform zeta potential measurements to elucidate the surface charge behaviors with respect to pH (Fig. 2.3). FAU exhibited a negatively charged surface for the entire pH range probably due to the dissociation of hydroxyl groups on terminal Si-OH and Al-OH groups present on the zeolitic surface [55]. Activated carbon exhibited two distinct regions. The first is a positive zeta potential at acidic pH levels up to 5.8. At pH values greater than 5.8, the activated carbon surface displays a negative zeta potential. The shift may be due to –OH, -CO and –COOH functional groups present in the surface, which bring about surface charges upon hydration [56]. The shift is also due to a conversion from a hydrophobic, positively charged H-type carbon to a hydrophilic, negatively charged L-type carbon [56]. A different isoelectric point than that of activated carbon was observed for CFAU. This results in an expansion of pH ranges at which the material exhibits a positive surface charge (pH < 8). On the other hand, the isoelectric point for Cu^{2+}-CFAU (W) shifts toward a pH of 8.5, which may be due to an unequal distribution of cations as that for CFAU. Ni^{2+}-CFAU (W) exhibited the same behavior as that of activated carbon. The surface of both composites ion exchanged in DMF remained neutral throughout the entire pH range.

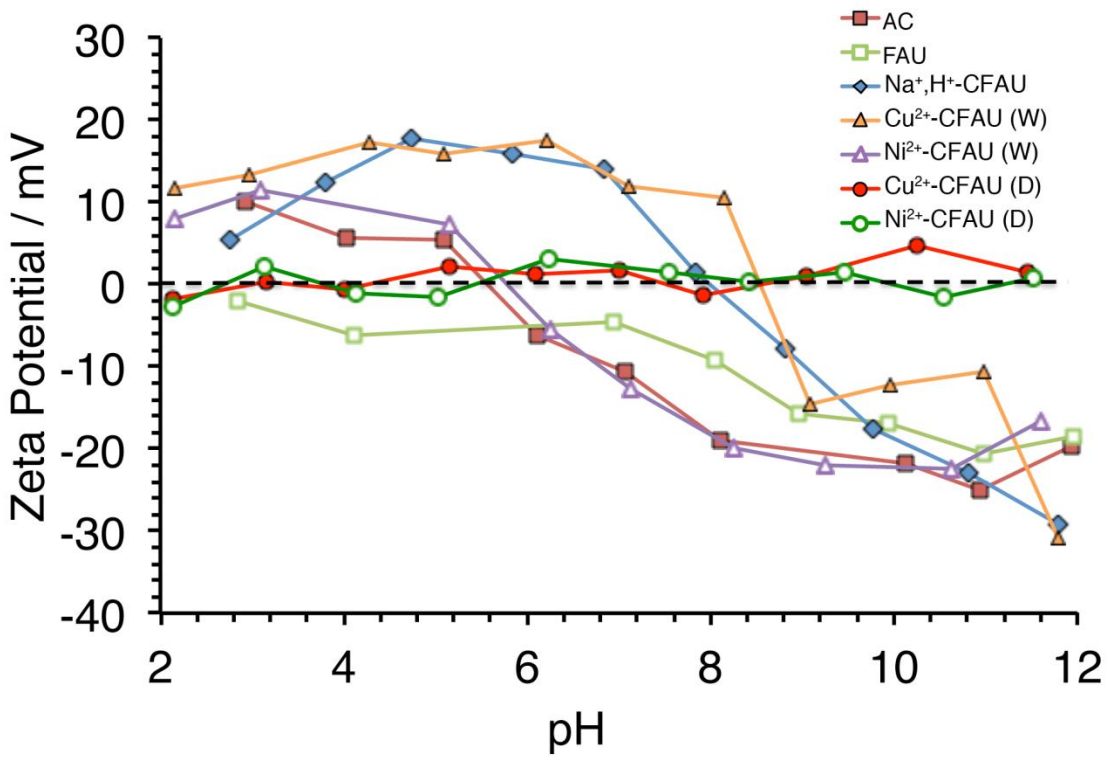

Figure 2.3 - Surface charge behavior of activated carbon (AC), detemplated CFAU, and transition metal (Cu^{2+} and Ni^{2+}) cation exchanged CFAU samples exchanged in either water (W) or dimethylformamide (D).

Salicylic acid adsorption uptake data gathered for detemplated CFAU were measured as a function of time at two initial concentrations of the adsorbate (Fig. 2.4). Equilibrium was reached after 3 hours at both initial concentration values and hence the 24 hours employed for the equilibrium tests were sufficient. The uptake profiles were each fitted with a slab-shape phenomenological model shown in the following equation:

$$F = 1 - \frac{2}{p^2}\sum_{n=1}^{\infty}\frac{1}{(n - 1/2)^2}\exp\left((-n - 1/2)^2 p^2 \frac{D_{AB}t}{L^2}\right) \qquad (2.4)$$

where F is the fractional uptake, t is the time and $D_{AB}L^{-2}$ is the diffusion time constant. Upon fitting of the model shown above, the resulting diffusion time constants were 0.136 and 0.455 min^{-1} for 1 and 8 ppm, respectively. As expected, the diffusion time constant

for 8 ppm is slightly larger than that for 1 ppm since, in very general terms, the concentration gradients will differ in order to satisfy Fick's first law of diffusion. However, both diffusion time constants are within the same order of magnitude suggesting that particle diffusion is dependent mostly on the adsorbent's structure rather than the sorbate molecule concentrations.

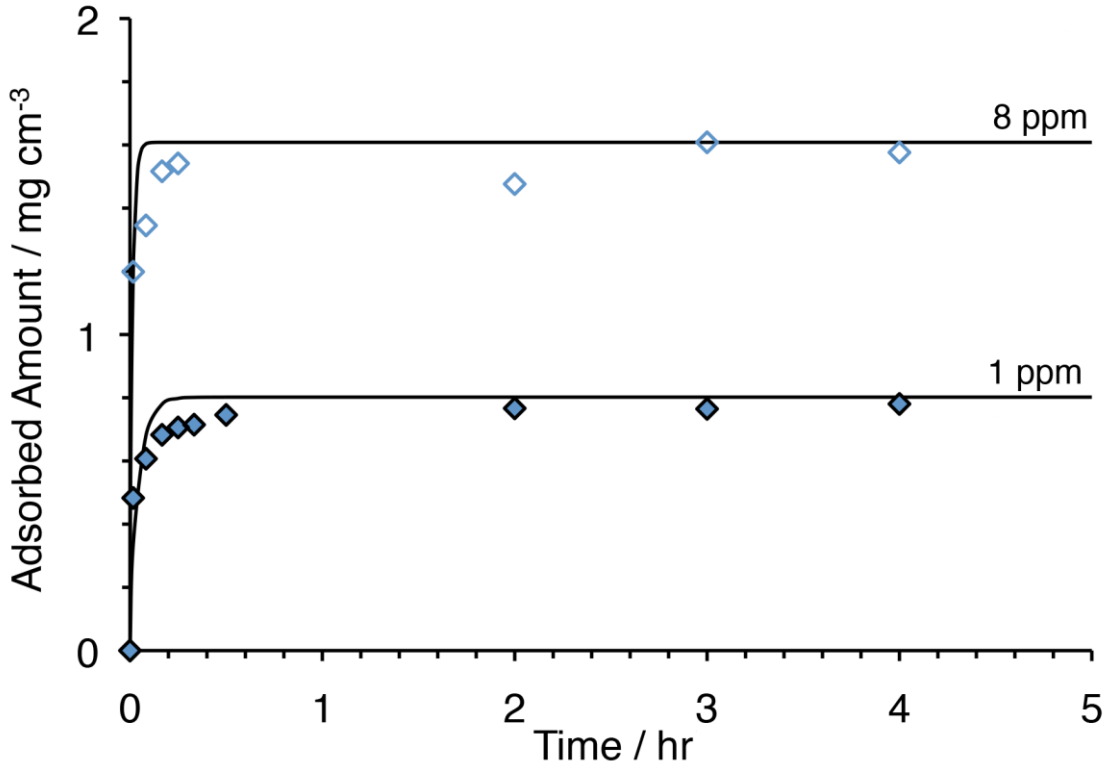

Figure 2.4 - Salicylic acid adsorption fractional uptake unto composite CFAU at 25 ˚C and nearly neutral pH for 1 ppm and 8 ppm initial concentrations. Solid line represents slab-shape phenomenological model fitting.

Salicylic acid adsorption equilibrium isotherm data gathered at 25 ˚C and nearly neutral pH are presented in Fig. 2.5. Adsorption quantities were normalized by volume instead of weight by means of each material density. Composite density was determined after carbon calcination in air by means of the mass fractions and densities of the individual materials, 1.9 and 0.31 g/cm^3, for Faujasite and activated carbon respectively,

resulting in a composite density of 1.2 g/cm^3. Theoretically, FAU growths within the mesopores and macropores of the activated carbon, hence there would be a considerable weight discrepancy between the activated carbon and the composites. Nonetheless, the composite would essentially occupy the same volume as activated carbon by itself; therefore it is more accurate to compare the two by means of the quantity of salicylic acid adsorbed by volume of adsorbent.

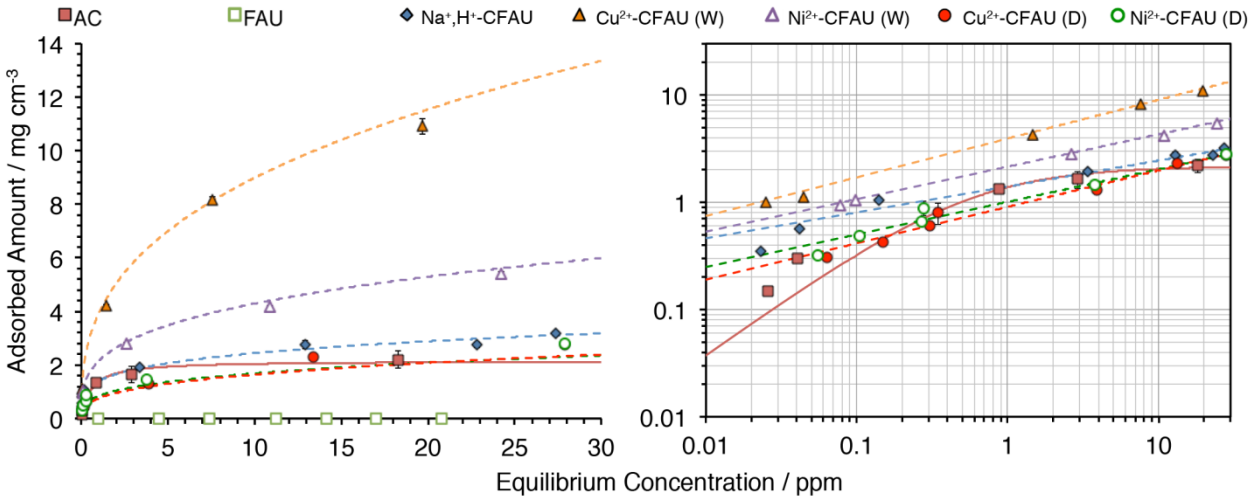

Figure 2.5 - Salicylic acid adsorption equilibrium isotherms for activated carbon (AC), sodium Faujasite (FAU), detemplated CFAU, and transition metal (Cu^{2+} and Ni^{2+}) cation exchanged CFAU samples exchanged in either water (W) or dimethylformamide (D) (*left*). Log-log plot of salicylic acid adsorption; data for Na-FAU has been omitted for clarity (*right*). All data were gathered at 25 ˚C and nearly neutral pH, in triplicates and contain error bars. Isotherms were fitted with the most suitable models: Langmuir for activated carbon (solid line) and Freundlich for the composites (dotted line).

In general, the adsorption capacity increases as follows: FAU < AC < Cu^{2+}-CFAU (D) ~ Ni^{2+}-CFAU (D) < Na^+,H^+-CFAU < Ni^{2+}-CFAU (W) < Cu^{2+}-CFAU (W). It should be noted that the salicylic acid molecule (pKa = 2.3) is deprotonated at nearly neutral pH conditions and, therefore, has an overall negative charge during the adsorption process. The molecular charge of salicylic acid and surface charge behavior for FAU (see Fig. 2.3) justifies the low to none adsorption of salicylic acid onto the zeolite. Since both the

adsorbate and adsorbent surface are negatively charged, electrostatic repulsion hinders the adsorption process. A similar observation might explain the adsorption capacity of activated carbon as well, however the vast difference in surface area of the zeolite when compared to that activated carbon (see Table 2.1) should suffice to enhance the adsorption. The materials exchanged in DMF exhibited a smaller adsorption capacity probably due to the lower surface area induced by the presence of DMF still in the structure and consequent blockage of available adsorption sites. CFAU outperformed activated carbon since the composite exhibited a positive surface charge at the working pH, the activated carbon component probably remained H-type and hydrophobic, and hence facilitated adsorption of the negatively charged salicylic acid.

The performance of the CFAU composites that were exchanged in water during the adsorption of the salicylic acid excelled that of all the other adsorbents. The salicylic acid uptake capacity increased probably due to both physical adsorption and complexation between the transition metal and aromatic ring of the adsorbate. However, Cu^{2+}-CFAU (W) distinctly outperformed all materials even at lower salicylic acid concentrations (Fig. 2.5). This is plausibly due be the larger quantity of Cu^{2+} present in the FAU component, resulting in more adsorption or complexation sites. Another possibility could be that Cu^{2+} occupies more accessible sites in the FAU structure than Ni^{2+}. Adsorption was so greatly enhanced for Cu^{2+}-CFAU (W) that yet another possibility to explain it would be that Cu^{+} cations instead of Cu^{2+} were present in the material. To increase stability of the cation, Cu^{+} can rearrange its electronic configuration to have an empty *s* and filled *d* orbitals. This rearrangement is ideal for complexation and would further enhance adsorption of

salicylic acid. XPS analysis was performed on the water-exchanged M^{n+}-CFAU samples in order to verify the aforementioned hypothesis (Fig. 2.6).

A nickel XPS spectrum exhibited a low intensity for the $2p_{3/2}$ peak at 855 eV that characterizes a Ni^{2+} oxidation state. On the other hand, Fig. 2.6 shows copper oxidation states distinguished by the Cu $2p_{3/2}$ peak at a binding energy range of 932-936 eV. Cu^{2+} is characterized by a binding energy within the range 933-936 eV and the appearance of shake-up satellites in the spectra at a higher binding energy (~ 944 eV), whereas Cu^{+} only exhibits a peak in the 932-933 eV range with no shake-up satellites [57, 58]. The lack of shake-up satellites suggests that copper might be present as Cu^{+} in Cu-CFAU (W), however the peaks occur at binding energies 933.17 eV and 934.05 eV, which correspond to tetrahedrally coordinated Cu^{2+} [58]. Therefore, it should be safe to assume that copper cations are present in CFAU in their divalent form.

Using the maximum experimentally observed salicylic acid adsorption loadings and the molecular weight of the Cu^{2+}-CFAU (W) unit cell (Table 2.1), the salicylic acid adsorption loading per unit cell would be 1.07 salicylic acid molecules adsorbed per unit cell. This value correlates well with what is expected, since due to the molecular size of salicylic acid (6.2 Å), only one molecule would fit within the FAU supercage.

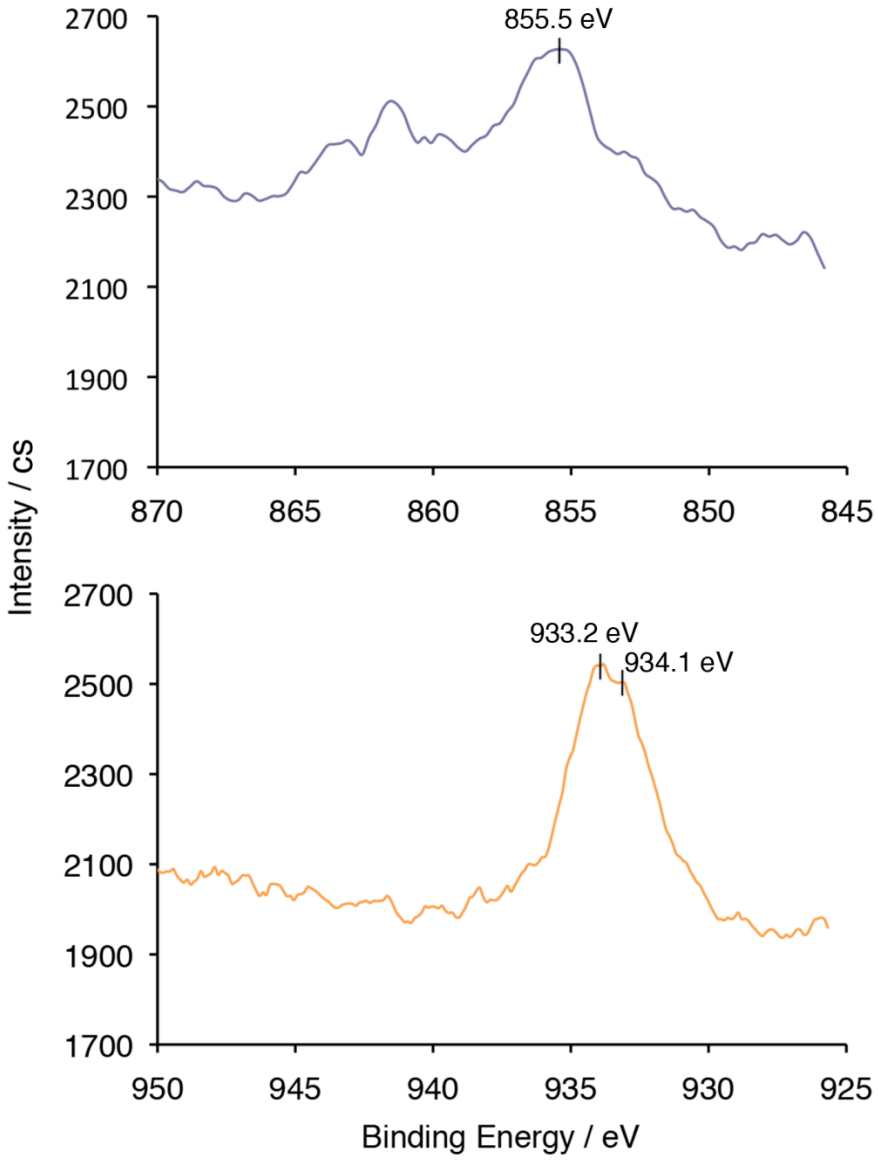

Figure 2.6 - XPS data for the Ni $2p_{3/2}$ peak for Ni^{2+}-CFAU (W) (*top*) and Cu $2p_{3/2}$ peak for Cu^{2+}-CFAU (W) (*bottom*).

Equilibrium adsorption isotherm data for each material were fitted with Langmuir, Freundlich or Sips isotherm models. Model parameters were estimated via a non-linear fit using equations (2.1), (2.2) and (2.3) and fit adequacy was evaluated with the residual root mean square error (RRMSE) (Table 2.2). Only activated carbon exhibited a clear adsorption saturation plateau. The composites all exhibited concave upward adsorption profiles, particularly Cu^{2+}-CFAU (W), which implies a rather strong

affinity between the adsorbate and adsorbent. Strong adsorbate-adsorbent interactions are also justified by the estimated Freundlich constant (K_F) values shown in Table 2.2 for which Cu^{2+}-CFAU (W) has the highest value. In general, RRMSE values suggest that Sips and Freundlich models are more adequate to describe the adsorption behavior in both activated carbon and the composites. However, further analysis of the corrected Akaike criterion (AIC_c) suggested that Langmuir and Freundlich are more suitable to model the adsorption isotherms of activated carbon and the composites, respectively. Fits for the aforementioned models can be observed by the solid and dotted line isotherms shown in Fig. 2.5. Uptake of salicylic acid onto activated carbon occurs only by physical adsorption onto the carbon's surface suggesting that the energy of adsorption would be the same at all surface sites as assumed by the Langmuir isotherm model. Salicylic acid uptake onto the composites also includes physical adsorption, but is enhanced due to the presence of a hydrophobic surface and electrostatic interactions influenced by the pH of the solution. Furthermore, for the transition metal exchanged composites (i.e., M^{n+}-CFAU), adsorption improved considerably due to interactions between the transition metals and the aromatic rings of the salicylic acid. The combinations of these mechanisms suggest that each adsorption site has a different energy associated to it, hence the heterogeneity factor (n_F) values greater than unity (Table 2.2).

Table 2.2 - Isotherm model parameters for salicylic acid adsorption onto different adsorbents.

Adsorbent	Isotherm Parameters												
	Langmuir				Freundlich				Sips				
	q_L (mg/g)	K_L (L/mg)	RRMSE	AICc	K_F ($mg^{(1-1/n)}L^{1/n}/g$)	n_F	RRMSE	AICc	q_S (mg/g)	K_S (L/mg)	n_s	RRMSE	AICc
AC	6.96	1.759	0.422	-2.356	3.578	3.88	0.787	5.126	7.80	1.202	1.46	0.256	1.642
Na^+, H^+-CFAU	2.28	4.296	0.258	-18.723	1.167	4.15	0.199	-30.746	4.62	0.371	2.81	0.162	-27.022
Cu^{2+}-CFAU (W)	10.74	0.313	0.635	2.558	3.263	2.77	0.177	-12.801	37.54	0.096	2.45	0.145	-5.188
Ni^{2+}-CFAU (W)	4.93	0.384	0.537	0.536	1.783	3.31	0.038	-31.100	92.01	0.020	3.21	0.046	-19.034
Cu^{2+}-CFAU (D)	2.17	0.604	0.331	-14.535	0.754	2.95	0.106	-32.711	92.01	0.008	2.91	0.123	-25.633
Ni^{2+}-CFAU (D)	2.02	1.387	0.331	-10.025	0.839	3.29	0.099	-26.905	92.01	0.009	3.21	0.115	-18.255

2.4 References

[1] S.A. Snyder, P. Westerhoff, Y. Yoon, D.L. Sedlak. Pharmaceuticals, personal care products, and endocrine disruptors in water: Implications for the water industry. Environ. Eng. Sci., 20 (2003) 449-469.

[2] B. Kasprzyk-Hordern, R.M. Dinsdale, A.J. Guwy. The removal of pharmaceuticals, personal care products, endocrine disruptors and illicit drugs during wastewater treatment and its impact on the quality of receiving waters. Water Res., 43 (2009) 363–380.

[3] M. Gros, M. Petrovic, A. Ginebreda, D. Barcelo. Removal of pharmaceuticals during wastewater treatment and environmental risk assessment using hazard indexes. Environ. Int., 36 (2010) 15-26.

[4] S.A. Snyder, M.J. Benotti. Endocrine disruptors and pharmaceuticals: Implications for water sustainability. Water Sci. Technol., 61 (2010) 145-154.

[5] A. Pal, K.Y.H. Gin, A.Y.C. Lin, M. Reinhard. Impacts of emerging organic contaminants on freshwater resources: Review of recent occurrences, sources, fate and effects. Sci. Total Environ., 408 (2010) 6062-6069.

[6] A. Jelic, M. Gros, A. Ginebreda, R. Cespedes-Sanchez, F. Ventura, M. Petrovic, D. Barcelo. Occurrence, partition and removal of pharmaceuticals in sewage water and sludge during wastewater treatment. Water Res., 45 (2011) 1165-1176.

[7] A. Jurado, E. Vazquez-Sune, J. Carrera, M.L. de Alda, E. Pujades, D. Barcelo. Emerging organic contaminants in groundwater in Spain: A review of sources, recent occurrence and fate in a European context. Sci. Total Environ., 440 (2012) 82-94.

[8] D.J. Lapworth, N. Baran, M.E. Stuart, R.S. Ward. Emerging organic contaminants in groundwater: A review of sources, fate and occurrence. Environ. Pollut., 163 (2012) 287-303.

[9] D.E. Vidal-Dorsch, S.M. Bay, K. Maruya, S.A. Snyder, R.A. Trenholm, B.J. Vanderford. Contaminants of emerging concern in municipal wastewater effluents and marine receiving water. Environ. Toxicol. Chem., 31 (2012) 2674-2682.

[10] M. Grassi, L. Rizzo, A. Farina. Endocrine disruptors compounds, pharmaceuticals and personal care products in urban wastewater: Implications for agricultural reuse and their removal by adsorption process. Environ. Sci. Pollut. Res., 20 (2013) 3616-3628.

[11] J.L. Liu, M.H. Wong. Pharmaceuticals and personal care products (PPCPs): A review on environmental contamination in China. Environ. Int., 59 (2013) 208-224.

[12] J. Rivera-Utrilla, M. Sanchez-Polo, M.A. Ferro-Garcia, G. Prados-Joya, R. Ocampo-Perez. Pharmaceuticals as emerging contaminants and their removal from water: A review. Chemosphere, 93 (2013) 1268-1287.

[13] X.L. Qu, J. Brame, Q.L. Li, P.J.J. Alvarez. Nanotechnology for a safe and sustainable water supply: Enabling integrated water treatment and reuse. Acc. Chem. Res., 46 (2013) 834-843.

[14] B. Ozkaya. Adsorption and desorption of phenol on activated carbon and a comparison of isotherm models. J. Hazard. Mater., 129 (2006) 158-163.

[15] M.S. Mauter, M. Elimelech. Environmental applications of carbon-based nanomaterials. Environ. Sci. Technol., 42 (2008) 5843-5859.

[16] L.F. Delgado, P. Charles, K. Glucina, C. Morlay. The removal of endocrine disrupting compounds, pharmaceutically activated compounds and cyanobacterial toxins during drinking water preparation using activated carbon: A review. Sci. Total Environ., 435–436 (2012) 509-525.

[17] S. Ghosh, A.Z.M. Badruddoza, K. Hidajat, M.S. Uddin. Adsorptive removal of emerging contaminants from water using superparamagnetic Fe_3O_4 nanoparticles bearing aminated β-cyclodextrin. J. Environ. Chem. Eng., 1 (2013) 122-130.

[18] Z. Hasan, E.J. Choi, S.H. Jhung. Adsorption of naproxen and clofibric acid over a metal-organic framework MIL-101 functionalized with acidic and basic groups. Chem. Eng. J., 219 (2013) 537-544.

[19] N.A. Khan, Z. Hasan, S.H. Jhung. Adsorptive removal of hazardous materials using metal-organic frameworks (MOFs): A review. J. Hazard. Mater., 244 (2013) 444-456.

[20] K.A. Cychosz, A.J. Matzger. Water stability of microporous coordination polymers and the adsorption of pharmaceuticals from water. Langmuir, 26 (2010) 17198-17202.

[21] S.M. Rivera-Jimenez, M.M. Lehner, W.A. Cabrera-Lafaurie, A.J. Hernandez-Maldonado. Removal of naproxen, salicylic acid, clofibric acid, and carbamazepine by water phase adsorption onto inorganic-organic-intercalated bentonites modified with transition metal cations. Environ. Eng. Sci., 28 (2011) 171-182.

[22] W.A. Cabrera-Lafaurie, F.R. Román, A.J. Hernández-Maldonado. Transition metal modified and partially calcined inorganic–organic pillared clays for the adsorption of salicylic acid, clofibric acid, carbamazepine, and caffeine from water. J. Colloid Interface Sci., 386 (2012) 381-391.

[23] V. Rakic, N. Rajic, A. Dakovic, A. Auroux. The adsorption of salicylic acid, acetylsalicylic acid and atenolol from aqueous solutions onto natural zeolites and clays: Clinoptilolite, bentonite and kaolin. Microporous Mesoporous Mater., 166 (2013) 185-194.

[24] W.A. Cabrera-Lafaurie, F.R. Román, A.J. Hernández-Maldonado. Single and multi-component adsorption of salicylic acid, clofibric acid, carbamazepine and caffeine from water onto transition metal modified and partially calcined inorganic–organic pillared clay fixed beds. J. Hazard. Mater., (2014) DOI: 10.1016/j.jhazmat.2014.1003.1009.

[25] J.E. Krohn, M. Tsapatsis. Phenylalanine and arginine adsorption in zeolites X, Y, and Beta. Langmuir, 22 (2006) 9350-9356.

[26] A. Rossner, S.A. Snyder, D.R.U. Knappe. Removal of emerging contaminants of concern by alternative adsorbents. Water Res., 43 (2009) 3787-3796.

[27] B. Koubaissy, G. Joly, I. Batonneau-Gener, P. Magnoux. Adsorptive removal of aromatic compounds present in wastewater by using dealuminated Faujasite zeolite. Ind. Eng. Chem. Res., 50 (2011) 5705-5713.

[28] D.J. de Ridder, J. Verberk, S.G.J. Heijman, G.L. Amy, J.C. van Dijk. Zeolites for nitrosamine and pharmaceutical removal from demineralised and surface water: Mechanisms and efficacy. Sep. Purif. Technol., 89 (2012) 71-77.

[29] A. Martucci, L. Pasti, N. Marchetti, A. Cavazzini, F. Dondi, A. Alberti. Adsorption of pharmaceuticals from aqueous solutions on synthetic zeolites. Microporous Mesoporous Mater., 148 (2012) 174-183.

[30] W.A. Cabrera-Lafaurie, F.R. Román, A.J. Hernández-Maldonado. Removal of salicylic acid and carbamazepine from aqueous solution with Y-zeolites modified with extraframework transition metal and surfactant cations: Equilibrium and fixed-bed adsorption. J. Environ. Chem. Eng., 2 (2014) 899-906.

[31] C. Adams, Y. Wang, K. Loftin, M. Meyer. Removal of antibiotics from surface and distilled water in conventional water treatment processes. J. Environ. Eng., 128 (2002) 253-260.

[32] P. Westerhoff, Y. Yoon, S. Snyder, E. Wert. Fate of endocrine-disruptor, pharmaceutical, and personal care product chemicals during simulated drinking water treatment processes. Environ. Sci. Technol., 39 (2005) 6649-6663.

[33] S.A. Snyder, S. Adham, A.M. Redding, F.S. Cannon, J. DeCarolis, J. Oppenheimer, E.C. Wert, Y. Yoon. Role of membranes and activated carbon in the removal of endocrine disruptors and pharmaceuticals. Desalination, 202 (2007) 156-181.

[34] Z. Yu, S. Peldszus, P.M. Huck. Adsorption of selected pharmaceuticals and an endocrine disrupting compound by granular activated carbon: 1. Adsorption capacity and kinetics. Environ. Sci. Technol., 43 (2009) 1467-1473.

[35] S.M. Rivera-Jimenez, A.J. Hernandez-Maldonado. Nickel(II) grafted MCM-41: A novel sorbent for the removal of naproxen from water. Microporous Mesoporous Mater., 116 (2008) 246-252.

[36] S.M. Rivera-Jimenez, S. Mendez-Gonzalez, A. Hernandez-Maldonado. Metal (M = Co^{2+}, Ni^{2+}, and Cu^{2+}) grafted mesoporous SBA-15: Effect of transition metal incorporation and pH conditions on the adsorption of naproxen from water. Microporous Mesoporous Mater., 132 (2010) 470-479.

[37] T. Frising, P. Leflaive. Extraframework cation distributions in X and Y Faujasite zeolites: A review. Microporous Mesoporous Mater., 114 (2008) 27-63.

[38] R.T. Yang, A.J. Hernandez-Maldonado, F.H. Yang. Desulfurization of transportation fuels with zeolites under ambient conditions. Science, 301 (2003) 79-81.

[39] R.T. Yang, Adsorbents: Fundamentals and applications, Wiley, New York, 2003.

[40] A.J. Hernández-Maldonado, R.T. Yang. Desulfurization of diesel fuels by adsorption via π-complexation with vapor-phase exchanged Cu (I)-Y zeolites. J. Am. Chem. Soc., 126 (2004) 992-993.

[41] J.E. Weder, C.T. Dillon, T.W. Hambley, B.J. Kennedy, P.A. Lay, J.R. Biffin, H.L. Regtop, N.M. Davies. Copper complexes of non-steroidal anti-inflammatory drugs: An opportunity yet to be realized. Coord. Chem. Rev., 232 (2002) 95-126.

[42] D. Kovala-Demertzi. Recent advances on non-steroidal anti-inflammatory drugs, NSAIDS: Organotin complexes of NSAIDS. J. Organomet. Chem., 691 (2006) 1767-1774.

[43] R. Cini, G. Tamasi, S. Defazio, M.B. Hursthouse. Unusual coordinating behavior by three non-steroidal anti-inflammatory drugs from the oxicam family towards copper(II). Synthesis, X-ray structure for copper(II)-isoxicam, -meloxicam and -cinnoxicam-derivative complexes, and cytotoxic activity for a copper(II)-piroxicam complex. J. Inorg. Biochem., 101 (2007) 1140-1152.

[44] K.Y. Foo, B.H. Hameed. The environmental applications of activated carbon/zeolite composite materials. Adv. Colloid Interface Sci., 162 (2011) 22-28.

[45] H.Y. Chen, J. Wydra, X.Y. Zhang, P.S. Lee, Z.P. Wang, W. Fan, M. Tsapatsis. Hydrothermal synthesis of zeolites with three-dimensionally ordered mesoporous-imprinted structure. J. Am. Chem. Soc., 133 (2011) 12390-12393.

[46] V.K. Jha, M. Matsuda, M. Miyake. Sorption properties of the activated carbon-zeolite composite prepared from coal fly ash for Ni^{2+}, Cu^{2+}, Cd^{2+} and Pb^{2+}. J. Hazard. Mater., 160 (2008) 148-153.

[47] M. Miyake, Y. Kimura, T. Ohashi, M. Matsuda. Preparation of activated carbon-zeolite composite materials from coal fly ash. Microporous Mesoporous Mater., 112 (2008) 170-177.

[48] B.A. Holmberg, H. Wang, J.M. Norbeck, Y. Yan. Controlling size and yield of zeolite Y nanocrystals using tetramethylammonium bromide. Microporous Mesoporous Mater., 59 (2003) 13-28.

[49] W. Fan, S. Shirato, F. Gao, M. Ogura, T. Okubo. Phase selection of FAU and LTA zeolites by controlling synthesis parameters. Microporous Mesoporous Mater., 89 (2006) 227-234.

[50] K.A. Cychosz, X. Guo, W. Fan, R. Cimino, G.Y. Gor, M. Tsapatsis, A.V. Neimark, M. Thommes. Characterization of the pore structure of three-dimensionally ordered mesoporous carbons using high resolution gas sorption. Langmuir, 28 (2012) 12647-12654.

[51] J. Huang, G. Wang, K. Huang. Enhanced adsorption of salicylic acid onto a β-naphthol-modified hyper-cross-linked poly (styrene-co-divinylbenzene) resin from aqueous solution. Chem. Eng. J., 168 (2011) 715-721.

[52] G. Horvath, K. Kawazoe. Method for the calculation of effective pore size distribution in molecular-sieve carbon. J. Chem. Eng. Jpn., 16 (1983) 470-475.

[53] S.U. Rege, R.T. Yang. Corrected horvath-kawazoe equations for pore-size distribution. AlChE J., 46 (2000) 734-750.

[54] I.J. Drake, Y.H. Zhang, D. Briggs, B. Lim, T. Chau, A.T. Bell. The local environment of Cu^{+} in Cu-Y zeolite and its relationship to the synthesis of dimethyl carbonate. J. Phys. Chem. B, 110 (2006) 11654-11664.

[55] T. Kuzniatsova, Y. Kim, K. Shqau, P.K. Dutta, H. Verweij. Zeta potential measurements of zeolite Y: Application in homogeneous deposition of particle coatings. Microporous Mesoporous Mater., 103 (2007) 102-107.

[56] H.L. Chiang, C.P. Huang, P.C. Chiang. The surface characteristics of activated carbon as affected by ozone and alkaline treatment. Chemosphere, 47 (2002) 257-265.

[57] M.C. Biesinger, L.W.M. Lau, A.R. Gerson, R.S.C. Smart. Resolving surface chemical states in XPS analysis of first row transition metals, oxides and hydroxides: Sc, Ti, V, Cu and Zn. Appl. Surf. Sci., 257 (2010) 887-898.

[58] D.Z. Yi, H. Huang, X. Meng, L. Shi. Adsorption-desorption behavior and mechanism of dimethyl disulfide in liquid hydrocarbon streams on modified Y zeolites. Appl. Catal., B., 148 (2014) 377-386.

Chapter 3

Synthesis of a Three-Dimensionally Ordered Mesoporous Carbon

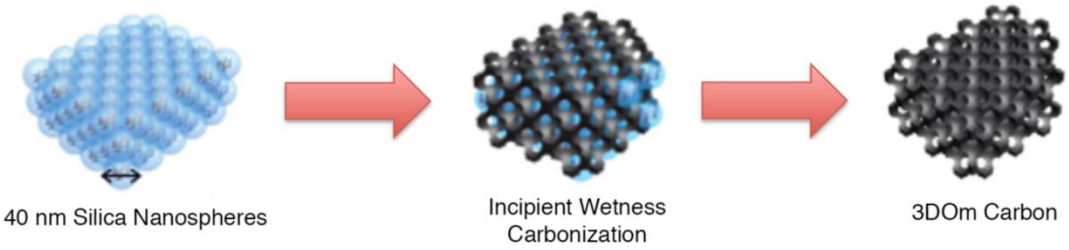

3.1 Introduction

The logical next step for composite synthesis would be the use of a three-dimensionally ordered mesoporous (3DOm) carbons. A 3DOm carbon would impart a higher level of structural order and uniformity for zeolite growth, which would result in a material with a well-defined pore size distribution containing both mesopores and macropores. Furthermore, mesopores could be tailored to the desired size depending on the diameter of the templates employed during the 3DOm carbon synthesis.

3.2 Experimental Section

3.2.1 Reagents and Materials

Reagents used for the 3DOm carbon synthesis were the following: L-lysine (98%), tetraethyl orthosilicate (TEOS, 98%), oxalic acid (98%), furfuryl alcohol (98%), potassium hydroxide (85%) and deionized water. All reagents, with the exception of deionized water, were purchased from Sigma-Aldrich.

3.2.2 Silica Nanoparticles Synthesis

Silica nanoparticles were synthesized according to the procedures outlined by Fan and coworkers [1]. An aqueous solution of L-lysine was prepared by dissolving L-lysine in deionized water. The solution temperature was brought to 90 °C and stirred. Tetraethyl orthosilicate (TEOS) was added dropwise and stirred for several hours in order for the following hydrolysis reaction to take place:

$$Si(OC_2H_5)_4 + 2\ H_2O \rightarrow SiO_2 + 4\ C_2H_5OH$$

The presence of the amino acid, L-lysine, in the solution is required since it acts as a catalyst for the above reaction; it also allows for a better control over the size of the particle due to interactions between the protonated amino group of the amino acid and the silicate. Finally, the hydrogen-bonding interactions between the L-lysine molecule facilitate the formation of a more ordered arrangement between the nanoparticles [2].

The final solution was transferred to a Teflon-lined stainless steel autoclave and kept at 100 °C under autogenous pressure for several hours. A 20 nm silica nanoparticle solution was obtained from the aforementioned procedure. These particles were utilized as seeds to synthesize 40 nm silica particles via a seeded growth technique. TEOS was added dropwise followed by hydrolysis for several hours. The procedure was carried out three times in order to augment the particle size to 40 nm. The final L-lysine-silica nanoparticle solution was evaporated in an oven at 70 °C. The final product was calcined in a furnace at 550 °C for several hours in order to remove the L-lysine.

3.2.3 3DOm Carbon Synthesis

The 40 nm silica particles prepared using the methods described above were used as templates for the synthesis of the 3DOm carbon through a process similar to the ones established

in the literature [2, 3]. A solution containing furfuryl alcohol and oxalic acid with a molar ratio of 200/1 was used to fill the space between the packed silica nanoparticles via an incipient wetness technique. It was determined that 0.62 mL of the furfuryl alcohol/oxalic acid solution per packed gram of silica nanospheres were required for proper impregnation. The product was heated to 90 °C under vacuum for 24 hours in order for the furfuryl alcohol to polymerize, and then placed under flowing nitrogen, first at 200 °C for a three hours to cure the polymer, and then at 900 °C for another three hours to carbonize the polymer. The product was then immersed in a 6M potassium hydroxide solution at 180 °C for three days in order to dissolve the template silica nanoparticles and yield the 3DOm carbon with 40 nm pores. The carbon was washed with copious amounts of deionized water and oven-dried.

3.3 Material Characterization

A Rigaku Ultima III diffractometer using CuKα radiation (λ = 1.5418 Å) operating at 40 kV and 44m fitted with a small angle module (SAXS) was utilized to characterize the 40 nm silica nanospheres. SAXS data demonstrated characteristic intensity peaks at 0.22°, 0.37° and 0.58° suggesting the successful synthesis of the 40 nm silica nanoparticles after comparison with patterns presented by Fan and coworkers (Fig. 3.1).

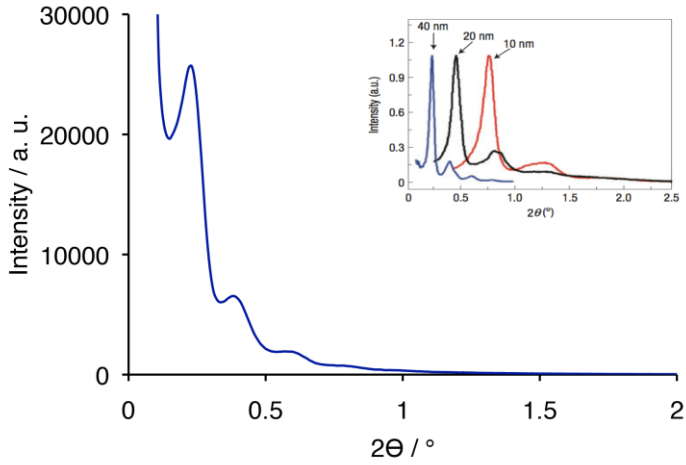

Figure 3.1-Small angle X-ray diffraction pattern for 40 nm silica nanospheres. Inset contains the diffraction data gathered by W. Fan and coworkers

In order to verify the textural properties of the 3DOm, nitrogen adsorption/desorption data were gathered at -196 °C using a Micromeritics ASAP 2020 static volumetric adsorption unit fitted with turbomolecular pumps. The resulting adsorption isotherm is compatible to a type IV classification with the corresponding hysteresis due to capillary condensation in the mesopores (Fig. 3.2).

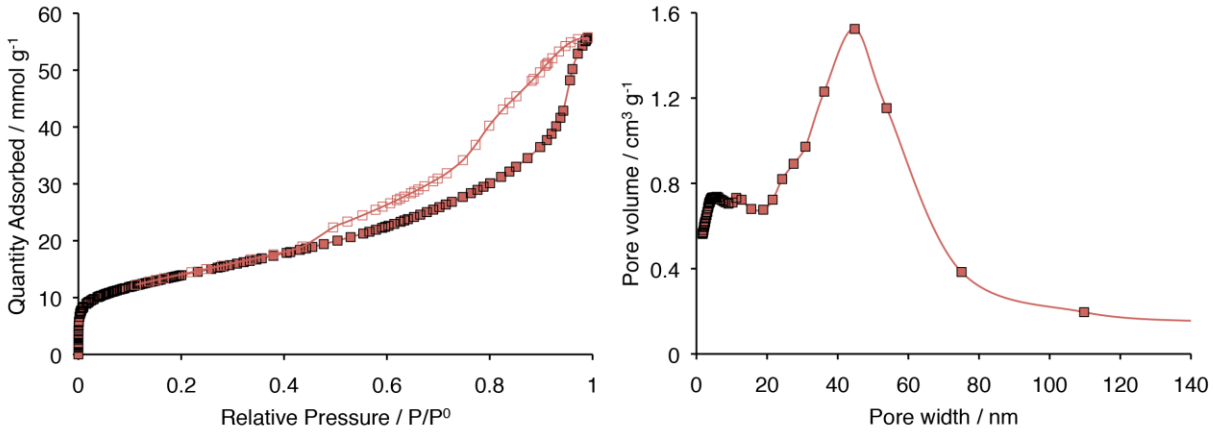

Figure 3.2 - Nitrogen equilibrium adsorption/desorption isotherm gathered at -196˚C for 40 nm 3DOm carbon (*left*). BJH adsorption pore size distribution curve for 3DOm carbon (*right*).

The isotherm and BET surface area of 1123 m^2/g correlated well with data published elsewhere [3, 4]. Pore size estimates were performed using the Barret-Joyner-Halenda (BJH) model with a Carbon Black STSA thickness curve and standard correction [5]. As observed in Fig. 3.2, the pore size distribution's largest peak occurs at 44.8 nm, which closely matches the silica nanospheres' expected 40 nm template diameter. The numerous left corner data points correspond to smaller micropores, suggesting that the porous structure is not completely uniform. However, these values should be treated as approximations since the BJH model assumes non-intersecting cylindrical pores rather than the spherical cage-like structures present in the 3DOm carbon [6].

3.4 References

[1] W. Fan, M.A. Snyder, S. Kumar, P.-S. Lee, W.C. Yoo, A.V. McCormick, R.L. Penn, A. Stein, M. Tsapatsis. Hierarchical nanofabrication of microporous crystals with ordered mesoporosity. Nat. Mater., 7 (2008) 984-991.

[2] T. Yokoi, Y. Sakamoto, O. Terasaki, Y. Kubota, T. Okubo, T. Tatsumi. Periodic arrangement of silica nanospheres assisted by amino acids. J. Am. Chem. Soc., 128 (2006) 13664-13665.

[3] K.A. Cychosz, X. Guo, W. Fan, R. Cimino, G.Y. Gor, M. Tsapatsis, A.V. Neimark, M. Thommes. Characterization of the pore structure of three-dimensionally ordered mesoporous carbons using high resolution gas sorption. Langmuir, 28 (2012) 12647-12654.

[4] H. Chen, J. Wydra, X. Zhang, P.-S. Lee, Z. Wang, W. Fan, M. Tsapatsis. Hydrothermal synthesis of zeolites with three-dimensionally ordered mesoporous-imprinted structure. J. Am. Chem. Soc., 133 (2011) 12390-12393.

[5] S. Lowell, J.E. Shields, M.A. Thomas, M. Thommes, Characterization of porous solids and powders: Surface area, pore size and density., Springer, The Neatherlands, 2006.

[6] R.T. Yang, Adsorbents: Fundamentals and applications., Wiley, New York, 2003.

Chapter 4

Conclusions and Future Work

A hierarchical porous carbon - M^{n+}[FAU] or M^{n+}-CFAU (M^{n+} = Ni^{2+} or Cu^{2+}; FAU = Y Zeolite) was synthesized and fully characterized. The composite exhibited great affinity toward salicylic acid (a CEC of high occurrence) over water due to a combination of the hydrophobic character of the carbon component and specific adsorbent-adsorbate interactions provided by a transition metal based Y zeolite. When tested against the individual activated carbon and zeolite, the CFAU composite excelled as an adsorbent throughout the whole concentration range tested. The overall adsorption capacities increased as follows: FAU < AC < Cu-CFAU (D) ~ Ni-CFAU (D) < CFAU < Ni-CFAU (W) < Cu-CFAU (W). Tailoring of an adsorbent to possess specific qualities enhances surface interactions as evidenced by the synergistic behavior between activated carbon and transition metal based zeolite, resulting in a hydrophobic, highly selective composite that could be an ideal platform to develop water treatment applications for the removal of CECs.

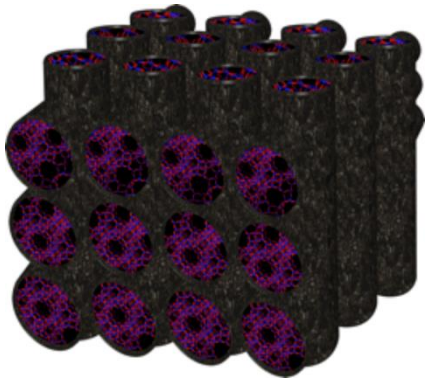

Figure 4.1 – Schematic representation of 3DOm carbon-Faujasite composite.

Future work should consist in evaluating CFAU composite performance in dynamic adsorption settings. Fixed-bed adsorption studies should be carried out for both single- and multi-component PPCP feeds for activated carbon, CFAU and transition metal exchanged CFAU to better model real-life conditions. In addition, composite synthesis and post-synthesis modifications should be performed with in-house 3DOm carbon (3DOm-CFAU) instead of activated carbon (Figure 4.1). The added uniformity of the 3DOm should impart control over the FAU structure. FAU crystals will be able to grow homogeneously within larger 40 nm pores, no void carbon area should result, and hence more active sites may be available for PPCP adsorption. Performance should also be assessed via both equilibrium and dynamic adsorption PPCP tests.

Appendix

Faujasite X-ray Diffraction Pattern

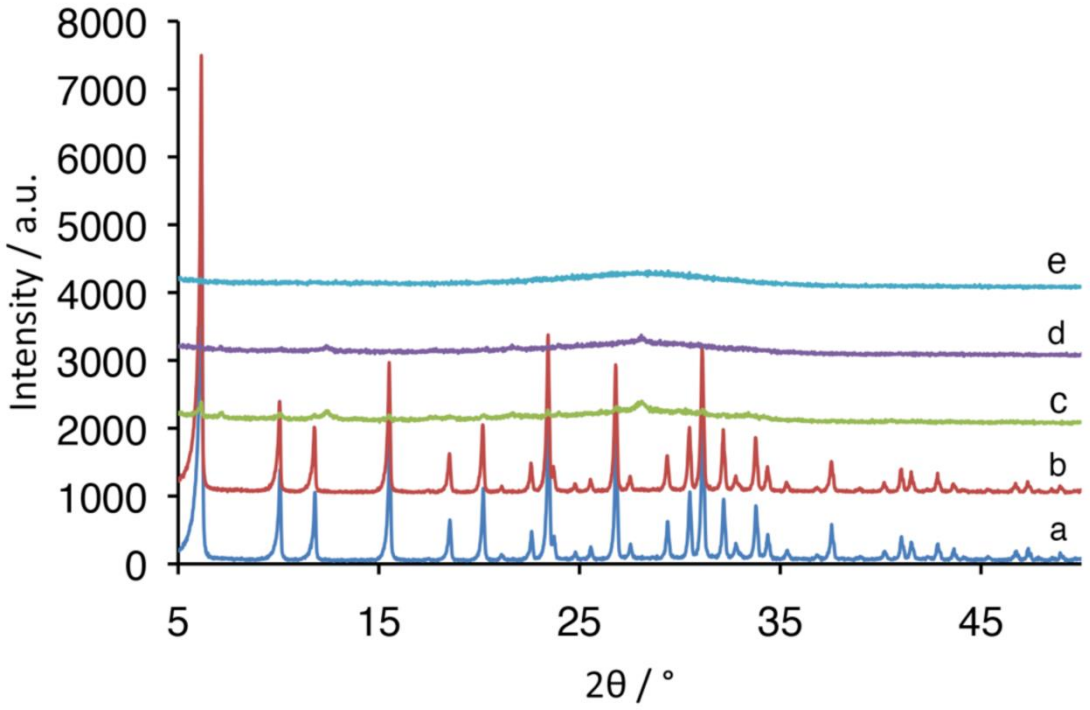

Figure A-1 - XRD patterns of commercially available sodium Faujasite (a), sodium Faujasite synthesized with Ludox HS-40 and 24 hour aging (b), silicic acid and 24 hour aging (c), Ludox HS-40 and 1 hour aging (d) and silicic acid and 1 hour aging (e).

Faujasite SEM

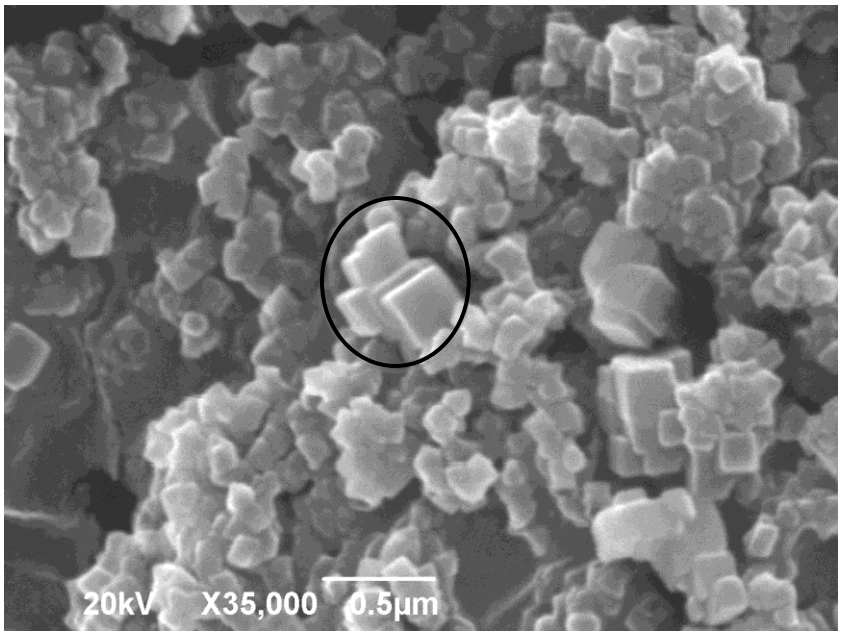

Figure A-2 – SEM image of Faujasite nanocrystals. Larger, cubic crystals (circled) correspond to an LTA impurity.